Title:

Pathogen invasion-dependent tissue reservoirs and plasmid-encoded antibiotic degradation boost plasmid spread in the gut

Authors:

Erik Bakkeren[1,2,3*], Joana A. Herter[1], Jana S. Huisman[4,5], Yves Steiger[1], Ersin Gül[1], Joshua P.M. Newson[1], Alexander O. Brachmann[1], Jörn Piel[1], Roland R. Regoes[4], Sebastian Bonhoeffer[4], Médéric Diard[6,7], Wolf-Dietrich Hardt[1*]

Affiliations:

[1]Institute of Microbiology, Department of Biology, ETH Zurich, Zurich, Switzerland
[2]Present affiliation: Department of Zoology, University of Oxford, Oxford, UK
[3]Present affiliation: Department of Biochemistry, University of Oxford, Oxford, UK
[4]Institute of Integrative Biology, Department of Environmental Systems Science, ETH Zurich, Zurich, Switzerland
[5]Swiss Institute of Bioinformatics, Lausanne, Switzerland
[6]Biozentrum, University of Basel, Basel, Switzerland
[7]Botnar Research Centre for Child Health, Basel, Switzerland

*for correspondence:
hardt@micro.biol.ethz.ch
erik.bakkeren@zoo.ox.ac.uk

Key words:

Plasmids, Salmonella, Antibiotic resistance, tissue reservoirs, persistence

Abstract:

Many plasmids encode antibiotic resistance genes. Through conjugation, plasmids can be rapidly disseminated. Previous work identified gut-luminal donor/recipient blooms and tissue-lodged plasmid-bearing persister cells of the enteric pathogen *Salmonella enterica* serovar Typhimurium (*S.*Tm) that survive antibiotic-therapy in host tissues, as factors promoting plasmid dissemination among *Enterobacteriaceae*. However, the buildup of tissue reservoirs and their contribution to plasmid spread await experimental demonstration. Here, we asked if re-seeding-plasmid acquisition-invasion cycles by *S.*Tm could serve to diversify tissue-lodged plasmid reservoirs, and thereby promote plasmid spread. Starting with intraperitoneal mouse infections, we demonstrate that *S.*Tm cells re-seeding the gut lumen initiate clonal expansion. ESBL plasmid-encoded gut luminal antibiotic degradation by donors can foster recipient survival under beta-lactam antibiotic treatment, enhancing transconjugant formation upon re-seeding. *S.*Tm transconjugants can subsequently re-enter host tissues introducing the new plasmid into the tissue-lodged reservoir. Population dynamics analyses pinpoint recipient migration into the gut lumen as rate-limiting for plasmid transfer dynamics in our model. Priority effects may be a limiting factor for reservoir formation in host tissues. Overall, our proof-of-principle data indicates that luminal antibiotic degradation and shuttling between the gut lumen and tissue-resident reservoirs can promote the accumulation and spread of plasmids within a host over time.

Main text:

Introduction:

The accumulation of antibiotic resistance genes in pathogenic bacterial strains is an important cause of antibiotic treatment failure. Conjugative antibiotic resistance plasmids are key drivers of this accumulation, accelerating the emergence of new bacterial strains genetically resistant to antibiotics (Wright, 2007). The mechanisms that contribute to the spread of resistance plasmids within an infected host are still not fully established.

Recently, we have begun assessing the spread of plasmids within bacteria colonizing or infecting mammalian hosts. In this work, when we refer to "host", we consistently refer to the mammalian host harbouring enteric bacteria. Plasmid spread within such hosts can be aided by tissue-lodged reservoirs of cells phenotypically recalcitrant to antibiotic therapy (Bakkeren et al., 2019). This process is called persistence and refers to a property of bacterial populations in which one subpopulation is killed by an antibiotic parallel to another subpopulation that is killed slowly ("persisters"), defined by phenotypic and not genotypic properties (Balaban et al., 2019; Gollan et al., 2019). Persisters can not only lead to antibiotic treatment failure, but they also have important implications for the evolution of antibiotic resistance (Levin-Reisman et al., 2017; Liu et al., 2020; Windels et al., 2019) or virulence (Bakkeren et al., 2020; Diard et al., 2014), and serve as long term reservoirs promoting the spread of resistance plasmids. We showed this using the model organism *Salmonella enterica* serovar Typhimurium (*S.*Tm) (Bakkeren et al., 2019). Invasive *S.*Tm cells form reservoirs of recalcitrant cells inside of host tissues (i.e., tissue persister reservoirs) that are difficult to treat with antibiotics (Bakkeren et al., 2019; Claudi et al., 2014; Diard et al., 2014; Helaine et al., 2014; Kaiser et al., 2014; Stapels et al., 2018). After treatment, these *S.*Tm cells can re-seed the gut lumen from their reservoirs along with any plasmids they carry. In the gut lumen, this re-seeding provides the plasmids with the opportunity to conjugate into new bacteria. Thereby, plasmids can subvert persisters to ensure long-term association within a given host. Besides persisters, *S.*Tm tissue invasion also creates an antibiotic susceptible subpopulation within the host tissues. In the absence of antibiotic therapy, the latter cells are generally more numerous than the persisters and are thought to drive chronic infections (Claudi et al., 2014; Kaiser et al., 2014; Lawley et al., 2008; Monack et al., 2004). Moreover, cells that constitute tissue reservoirs during chronic infection are known to re-seed the gut lumen over time (Lam & Monack, 2014). However, the role of this second, non-persister, tissue-lodged pathogen population in plasmid dissemination remained to be formally established.

Although very specific characteristics define antibiotic persistence (i.e., biphasic killing curves defining the susceptible and tolerant subpopulations) (Balaban et al., 2019), there are many similarities to persistent (aka long-term, chronic) infection. Numerous bacterial pathogens can survive or evade host immune defenses and antibiotics alike in a recalcitrant state (e.g. *Pseudomonas aeruginosa, Escherichia coli, Staphylococcus aureus,* or *Salmonella enterica*) (Bakkeren et al., 2020; Gollan et al., 2019; Grant & Hung, 2013). Using mouse models, tissue reservoirs of *S.*Tm antibiotic persisters located in the intestinal mucosa or systemic sites can re-seed the gut lumen after the cessation of antibiotic therapy (Bakkeren et al., 2019; Diard et al., 2014; Endt et al., 2012; Kaiser et al., 2014; Onwuezobe et al., 2012). In chronically infected hosts, the pathogen population tends to diversify forming non-growing and growing subpopulations which are kept in check by immune defenses, but can rise upon neutralization of cytokines (e.g. IFNγ or TNFα) (Monack et al., 2004; Pham et al., 2020). During monoclonal infections characteristic of many experimental models, intraspecies priority effects from *S.*Tm colonizing a given site within the host reduce the chances of colonization by pathogen cells that are arriving later (Lam & Monack, 2014). However, gut colonization is rarely a monoclonal process. Examples of multiple *Enterobacteriaceae* strains co-

occuring in the same host have been demonstrated in longitudinal clinical studies monitoring fecal *Enterobacteriaceae* populations, but also shown in swine where different strains of *Salmonella* colonize the lymph nodes compared to the gut lumen (Leon-Sampedro et al., 2021; Martinson et al., 2019; San Roman et al., 2018; Tenaillon et al., 2010). Based on these considerations, we hypothesized that repeated re-seeding and re-invasion events during persistent infection may promote plasmid spread. Here, we define "re-seeding" as cells exiting tissue reservoirs into the gut lumen, and "re-invasion" as cells entering tissue reservoirs from the gut lumen.

Finally, we reasoned that certain resistance plasmids should themselves expedite re-seeding-transfer-invasion cycles within the infected host. In particular, this should pertain to plasmid-encoded resistance genes encoding enzymes degrading antibiotics with an extra-cytoplasmic target (e.g. beta-lactamases). Extended spectrum beta-lactamases (ESBL) capable of hydrolyzing a wide variety of beta-lactam antibiotics including ampicillin and cephalosporins, are of particular concern, as beta lactam antibiotics account for about 2/3 of the antibiotics deployed annually worldwide (WHO, 2017). These periplasmic enzymes may facilitate re-seeding of sensitive recipients, as resistance plasmids encoding beta-lactamases are able to reach high density under beta-lactam treatment, and clear the local environment from antibiotics, as shown *in vitro* (Perlin et al., 2009). However, it had remained unclear if such donor-mediated reduction of local beta-lactam concentrations would suffice for promoting survival of susceptible recipients *in vivo*, fostering plasmid transfer and subsequent reservoir formation in the host's tissue.

To address this, we quantitatively assessed the link between within-host plasmid transfer, invasion-reservoir formation-re-seeding cycles and plasmid accumulation in the host's tissues using *S.*Tm mouse models for both antibiotic persistence and chronic infection. To study these processes in a proof-of-concept approach, we chose donor-recipient-plasmid combinations featuring a high conjugation efficiency and relieved potential restrictions to conjugation or reservoir formation in the mouse gut like colonization resistance conferred by the microbiota, and priority effects of strains that already colonize tissue reservoirs. Thereby, we could demonstrate expansion of the plasmid diversity in the gut tissue reservoir, a role for the chronically infecting *S.*Tm subpopulation and the effect of gut luminal antibiotic degradation by beta-lactamase expressing donor strains.

Results:

Plasmids that enter *S.*Tm in the gut lumen can be stored in intestinal tissue reservoirs

To study plasmid transfer within a host and its subsequent storage in the host tissues, we modified a mouse model from our previous work (Bakkeren et al., 2019). For most plasmid transfer experiments, we used the IncI1 plasmid P2 (a close relative of extended-spectrum beta-lactamase (ESBL) plasmids; also known as pCol1b9), which naturally occurs in *S.*Tm SL1344 and spreads in the gut of antibiotic pretreated mice and during diet-elicited *Enterobacteriaceae* blooms (Bakkeren et al., 2021; Bakkeren et al., 2019; Diard et al., 2017; Moor et al., 2017; Stecher et al., 2012; Wotzka et al., 2019).

For all experiments, we used streptomycin resistant derivatives of *S.*Tm ATCC 14028S that naturally do not contain P2 as recipient strains. We infected 129/SvEv mice intraperitoneally (i.p.) with recipients to allow the formation of tissue reservoirs of *S.*Tm (**Fig. 1A**; left side, green) (Bakkeren et al., 2019). The advantage of this i.p. infection model is three-fold. First, it allows us to study plasmid transfer and subsequent tissue storage in models for antibiotic persistence (the focus of (Bakkeren et al., 2019)) and to extend the work to persistent infection (this work). This is attributable to the capacity of the *Nramp1*-positive 129/SvEv mice to limit systemic pathogen growth, as shown previously in chronic infections initiated via the intravenous or the oral route (Cunrath & Bumann, 2019; Monack et al., 2004). Second, i.p. infection bypasses the need for gut colonization, ensuring

150 that plasmid transfer observed later in the experiment is truly a result of plasmid conjugation into
151 recipients entering from tissue reservoirs into the gut lumen. Third, the i.p. infection model mimics
152 tissue reservoirs that are established after systemic spread following gut colonization (and therefore
153 allows us to study the role of persistent infection in plasmid transfer dynamics) (Bakkeren et al.,
154 2019; Lam & Monack, 2014; Monack et al., 2004; Stecher et al., 2006). Notably, our model differs
155 from established persistent infection models in which infections are established for >28 days from an
156 oral inoculation (Monack et al., 2004). However, to allow us to investigate re-seeding with high
157 sensitivity, it was important to keep the gut lumen free of the initial recipient (without using
158 antibiotics). We would like to point out a caveat of this i.p. model, in that it eliminates the
159 contribution of priority effects attributable to the inoculation route. As natural infections would
160 occur via the oral colonization route, sites that are normally occupied by invading *S.*Tm cells (e.g. the
161 mesenteric lymph node; mLN) are less colonized after an i.p. infection compared to an oral infection.
162 This means that invasion events from the gut luminal side later in the experiment are likely over-
163 estimated in this model. On the other hand, this provides us with an exquisitely sensitive system to
164 ask if tissue re-invasion can in principle expand the plasmid reservoirs within a host.
165 Next, we treated mice with a dose of streptomycin to suppress the microbiota and allow
166 colonization of P2^{cat} carrying donor strains (Sm^{R}) introduced orally (**Fig. 1A**, blue). Note that both the
167 donors and recipient strains used in this experimental model are streptomycin resistant. Therefore,
168 the systemic infection by the recipients is unaffected by the antibiotic and the recipients can grow
169 upon re-seeding of the gut lumen (= persistent systemic infection model). As the donor, we used a
170 derivative of *S.*Tm SL1344 that lacks functional type 3 secretions systems (TTSS)-1 and -2 (*invG* and
171 *ssaV* mutant; SL1344^{Avir}) (Hapfelmeier et al., 2005). This prevented invasion of the *S.*Tm donors into
172 tissues to exclude tissue-localized plasmid transfer. We used SL1344 derivatives to study interactions
173 between different strains of bacteria, rather than isogenic strain interactions that would limit co-
174 existence of donors and recipients in the gut after re-seeding (Lam & Monack, 2014; Lee et al., 2013).
175 Feces were monitored over time to investigate plasmid transfer dynamics and mice were euthanized
176 at day 10 post infection to assess the formation of new intra-cellular plasmid reservoirs by recipients
177 that had obtained a plasmid (transconjugants; **Fig. 1A**, red).
178 One day after the addition of donors (SL1344^{Avir} P2^{cat}), recipients started re-seeding into the
179 gut lumen and transconjugants were detected in the feces (**Fig. 1B, Fig. 1-figure supplement 1A**). By
180 day 10 of the experiment, transconjugants were detected in the majority of mice (8/13 mice; **Fig. 1B**).
181 We confirmed plasmid transfer had occurred by performing PCRs with both plasmid- and recipient-
182 specific primers (**Fig. 1-figure supplement 2).** Re-seeding and plasmid acquisition depended on the
183 TTSS-2 encoded on *Salmonella* pathogenicity island (SPI)-2, as recipients lacking a functional TTSS-2
184 (14028S *ssaV* mutant; *S.*Tm^{SPI-2}) failed to re-seed frequently, and consequently transconjugants were
185 rarely observed (1/8 mice; **Fig. 1B. Fig. 1-figure supplement 1B**). Their failure to establish substantial
186 tissue reservoir sizes (e.g. in the spleen, liver, or gall bladder) could explain the limited re-seeding of
187 *S.*Tm^{SPI-2} (**Fig. 1C**). However, re-seeding was not dependent on the TTSS-1 encoded on SPI-1, as
188 mutant recipient strains that lack a functional TTSS-1 apparatus (14028S *invG* mutant; *S.*Tm^{SPI-1})
189 established tissue reservoirs and re-seeded the gut (**Fig. 1-figure supplement 3)**. Furthermore, we
190 performed a control experiment to exclude the contribution of donor strains themselves to the re-
191 seeding process of recipients. To this end, we performed the same experiment as in **Fig. 1A**, but in
192 parallel included a control group where donors were not added. Re-seeding was detected in both
193 groups (2/4 mice with donors; 3/5 mice without donors by day 10 of the experiment), indicating that
194 the presence of donors did not promote re-seeding (**Fig. 1-figure supplement 4**).
195 Altogether, these results indicated that bacteria re-seeding from tissue reservoirs can gain
196 plasmids in the gut. In contrast to previous work (Bakkeren et al., 2019) this occurred without
197 previous selection for persister sub-populations. Performing our experiments in the absence of
198 antibiotic treatment to select for persisters allowed us to assess the contribution of growing tissue-

199 lodged pathogen subpopulations. Importantly, we analyzed here if the gut luminal plasmid was
200 carried back into host tissues by transconjugants. Indeed, transconjugants were detected in the
201 mLNs of mice where gut luminal plasmid transfer was observed. Occasionally such transconjugants
202 were also observed in other tissue reservoirs such as the spleen and liver associated with further
203 systemic spread after tissue invasion (**Fig. 1C**).
204 Next, we tested if this process could be generalized to other donors colonizing the gut lumen.
205 For this, we used *E. coli* 536 carrying P2^{cat} as a donor. This strain is naturally streptomycin resistant
206 and colonizes the streptomycin-pretreated mouse gut for long periods of time (Brzuszkiewicz et al.,
207 2006; Ghalayini et al., 2019). Also in this case, re-seeding of *S.*Tm 14028S recipients occurred
208 followed by the formation of transconjugants in the majority of the mice (7/12 mice) (**Fig. 1D, Fig. 1-**
209 **figure supplement 1C**). Once again, re-seeding and conjugation was associated with the formation of
210 new plasmid tissue reservoirs by invading transconjugants, primarily in the mLN (**Fig. 1E**). To assess if
211 our i.p. infection experimental model allowed the comparison between both persistent infection and
212 antibiotic persistence, we performed a control experiment in which we treated mice three times with
213 ceftriaxone 2 days after i.p. infection to select for persisters (**Fig. 1-figure supplement 5**), as done
214 previously (Bakkeren et al., 2019). After the addition of *E. coli* 536 P2^{cat} donors, *S.*Tm^{WT} recipients
215 began to re-seed in some mice. However, this occurred later and in a smaller number of the analyzed
216 mice, as antibiotic persisters are much less abundant (and need to re-enter growth) compared to the
217 much larger population of persistently infecting *S.*Tm^{WT} recipient cells. Regardless, this re-seeding
218 was also associated with plasmid transfer and the occasional formation of tissue reservoirs of
219 transconjugants in the mLN (**Fig. 1-figure supplement 5**).
220 Altogether, our data demonstrates that plasmids can subvert both *S.*Tm derived from tissue
221 lodged populations of antibiotic persisters, or from persistent infections. Cells from either type of
222 tissue lodged population can re-enter the gut lumen and serve as recipients in interbacterial
223 interactions. This process can be followed by reinvasion forming new tissue reservoirs, capturing a
224 record of conjugative plasmids that had previously been present in the gut lumen.
225
226 **Re-seeding of the gut lumen, plasmid transfer, and the formation of new reservoirs is limited by**
227 **the gut luminal carrying capacity and the conjugation rate**
228
229 Next, we examined the dynamics of pathogen-assisted plasmid transfer and storage. This
230 should identify bottlenecks and inform about the possible routes that recipients and transconjugants
231 take to exit and re-enter host tissues in more detail. First, we explored possible sources of
232 persistently infecting recipients that re-seed the gut lumen by characterizing the localization of *S.*Tm
233 in tissue reservoirs. We infected mice i.p. with *S.*Tm 14028S recipients and euthanized mice 2 days
234 later, while keeping the gut luminal microbiota intact (at the time point when normally the donors
235 are added). As expected based on previous work (Bakkeren et al., 2019; Grant et al., 2008; Hensel et
236 al., 1995; Lam & Monack, 2014; Monack et al., 2004), *S.*Tm were found in the spleen, liver, and
237 kidney at high density (**Fig. 1-figure supplement 6**), which likely occurred because of blood flow to
238 these organs immediately after i.p. infection of *S.*Tm (Grant et al., 2008). Although bacteria were not
239 detected in the feces (our readout for re-seeding), *S.*Tm was found in the content of the small
240 intestine (i.e. primarily the jejunum and ileum, but also the duodenum), and this was correlated with
241 *S.*Tm in the tissues of these sites (**Fig. 1-figure supplement 6**). Furthermore, we found high densities
242 of *S.*Tm in the lining of the small intestinal tissues that contains the gut-associated tissues such as
243 Peyer's patches (here called small intestinal gut associated lymphoid tissues; S.I. GALT). The gall
244 bladder contained some *S.*Tm, but the low densities suggest that the gall bladder is not the primary
245 route of re-seeding in this model (as suggested in some other experimental models (Lam & Monack,
246 2014)). Future work may address if *S.*Tm re-seeds from the small intestinal tissues after spread from
247 blood or lymphatic supply.

248 Instead, we focused on the dynamics of re-seeding followed by plasmid transfer into this
249 luminal pathogen population and asked in which conditions this occurs. We mixed equal ratios of
250 recipient strains harbouring three different sequence-tagged barcodes at a neutral location in the
251 chromosome (14028S Sm^R *TAG1-3*; 1:1:1 ratio) and i.p. infected mice (same mice as in **Fig. 1B**). As
252 donor strains, we used $SL1344^{Avir}$ containing P2 labelled with four additional unique sequence tags
253 ($P2^{TAG4-7}$; 1:1:1:1 ratio). All tags can be identified using quantitative PCR (Grant et al., 2008). At the
254 end of the experiment, we analyzed the ratio of each of these tags in the recipient population
255 (enriching for recipients = recipients + transconjugants) by qPCR. We plotted the relative proportion
256 of each tag relative to all tags (both chromosomal and recipient tags) to preserve information about
257 the proportion of plasmid tags within the recipient population. To visually correlate re-seeding of
258 *S.*Tm into the gut lumen with the localization of these tags in tissue reservoirs, we sorted and color-
259 coded the tags according to the most abundant tag in the feces. While chromosomal tags were
260 evenly distributed in primary tissue reservoirs (e.g. spleen and liver), the feces were typically
261 dominated by just one of the three tagged strains, implying a narrow population bottleneck (**Fig. 2A,**
262 **Fig. 2-figure supplement 1**). Thus, re-seeding from these tissue reservoirs is a rare process that is
263 followed by clonal expansion. We also analyzed the gall bladder as a possible source of re-seeding,
264 and the mLN as a site where new tissue reservoirs are formed after reinvasion of re-seeding *S.*Tm.
265 Although the chromosomal tags were slightly more skewed in the gall bladder compared to the
266 spleen and liver, there was no correlation between the rank of the tags found in the feces and in the
267 gall bladder (**Fig. 2A, Fig. 2-figure supplement 1A**; e.g. mouse 7 contains different most abundant
268 tags in the feces and gall bladder). Interestingly, the mLN and the feces typically shared the same
269 most abundant chromosomal tag (~10-fold median reduction of the proportion of the most and
270 second most abundant tag in the feces; **Fig. 2A**), suggesting that re-seeding followed by re-invasion
271 could be skewing this distribution, rather than a bottleneck in cells spreading to the mLN after the
272 i.p. injection. Note that the mLN population likely reflects the population that has invaded into the
273 gut tissue. However, due to unavoidable background contamination from separating the gut tissue
274 from the gut lumen, we chose to examine the mLN instead. The correlation between mLN and fecal
275 chromosomal tags was not seen in one mouse (mouse 9 in **Fig. 2-figure supplement 1A**), in which
276 recipients were not found at high densities in the feces, further supporting the hypothesis that the
277 distribution of tags in the mLN is heavily influenced by re-invading cells from the gut lumen. We
278 plotted the plasmid tags found in the transconjugant population in the same manner (**Fig. 2B**). In
279 mice where plasmid transfer was detected (population sizes in **Fig. 1-figure supplement 1A**; raw tag
280 data in **Fig. 2-figure supplement 1**), almost all plasmid tags were found, although their distribution
281 was skewed (**Fig. 2B**). Importantly, the plasmid tags found in the feces were mostly also found in the
282 mLN, implying that plasmids were carried into the mLN by transconjugants that had formed in the
283 gut lumen (**Fig. 2B**). In addition, the data indicated that mLN entry of the plasmid-bearing
284 transconjugants occurred more than once in most of the mice.
285 As a control, we also analyzed the extent to which the presence of donors in the gut lumen
286 contributed to the rarity of re-seeding, analyzing the 7 chromosomal tags contained in the recipient
287 population of mice in **Fig. 1-figure supplement 4.** We found that one or few tags dominated the
288 population in the feces in both mice with or without donors, indicating that the presence of donors
289 did not have a detectable effect on the low re-seeding frequency (**Fig. 2-figure supplement 2**).
290 Next, we developed a mathematical model (**Supplementary information**) to explore the
291 relative contribution of re-seeding (migration rate; μ) and plasmid transfer (conjugation rate per
292 mating pair; donor or transconjugant to recipient; γ) to the bacterial dynamics. We fit the model to
293 the experimental data (evenness of tags in **Fig. 2A-B**; recipient and transconjugant population sizes in
294 **Fig. 1-figure supplement 1A**; **Supplementary information**) to reveal the most likely migration and
295 conjugation rates (**Fig. 2C** in red; μ = 1.78 recipient CFU/g feces per day; $\gamma = 3.16\times10^{-11}$ events per
296 CFU/g feces per day; **Supplementary table S2**). This corresponds to an average per-recipient rate of

297 migration vs conjugation (μ, γ) of 2.1 x 10^{-6} per day (by dividing μ with the recipient population in
298 host tissue reservoirs) or 3.2 x 10^{-2} per day respectively (by multiplying γ with the gut luminal donor
299 population; **Supplementary information**). This identified recipient re-seeding as the rate limiting step
300 in our observed plasmid transfer dynamics, although the conjugation rate influenced the evenness of
301 the plasmid tags and the time until recipients were converted into transconjugants (**Fig. 2-figure**
302 **supplement 3**). In our experimental system, we used streptomycin to decrease colonization
303 resistance, effectively raising the carrying capacity (parametrized at 10^9 CFU/g feces for **Fig. 2C, Fig.**
304 **2-figure supplement 3**). However, since conjugation is density dependent, we reasoned that the level
305 of colonization resistance should influence our results. To test the range of *Enterobacteriaceae*
306 densities that would allow appreciable densities of transconjugants (e.g. sufficient to allow invasion
307 into new tissue reservoirs), we fixed the migration and conjugation rates to the most likely values
308 from **Fig. 2C** (i.e., μ = 1.78 recipient CFU/g feces per day; γ = 3.16×10^{-11} events per CFU/g feces per
309 day)**.** We then varied the carrying capacity as a proxy for colonization resistance, using the
310 population sizes of recipients and transconjugants at the end of the experiment (day 10) as a
311 readout. While recipient densities increased proportionally to the carrying capacity, the
312 transconjugant population size remained below 10^6 CFU/g feces until the carrying capacity reached
313 10^7 - 10^8 CFU/g feces (**Fig. 2D;** grey dotted lines). To validate this with our experimental data, we re-
314 analyzed the experimental data from **Fig. 1B-E** (pooling data from both *S.*Tm^{Avir} and *E. coli* donors),
315 correlating the donor population size at day 10 of the experiment (as a proxy for colonization
316 resistance) with the transconjugant populations in both the feces and the mLN at day 10 (**Fig. 2-**
317 **figure supplement 4A-B)**. As suggested by our model, transconjugant formation and re-invasion was
318 more likely in mice that harboured higher gut luminal donor densities, indicating a reduction in
319 colonization resistance (**Fig. 2-figure supplement 4A-B**). We confirmed this trend in simulations with
320 both a higher and lower conjugation rate than in our experimental system (**Fig. 2-figure supplement**
321 **4C-D**). A plasmid with a higher conjugation rate was found to be less inhibited by colonization
322 resistance. It could rise to appreciable densities (e.g. >10^6 CFU/g) even with lower overall carrying
323 capacities. Altogether, our data suggest a critical role for colonization resistance in limiting tissue-
324 reservoir-assisted plasmid spread dynamics, but also highlights the role of the plasmid transfer rate
325 defined by the plasmid-strain association.
326
327 **Plasmids can use re-invading *S.*Tm to form a persistent tissue reservoir that survives antibiotics and**
328 **permits spread to further strains in the gut post-antibiotic treatment**
329
330 We then addressed the implications of newly formed plasmid tissue reservoirs for future
331 plasmid transfer dynamics in the gut. For this, in the first phase of the experiment, we performed the
332 same experiment as in **Fig. 1D** (using *S.*Tm 14028S Sm^R as a recipient and *E. coli* 536 P2^{cat} as a donor),
333 but on day 10 we gave mice three doses of ciprofloxacin instead of stopping the experiment (second
334 phase of the experiment; **Fig. 3A**). As before, *S.*Tm re-seeded from tissue reservoirs, obtained a
335 plasmid in the gut lumen, and transconjugants carried the plasmid into host tissues (i.e. mLN) before
336 the ciprofloxacin treatment killed gut luminal populations and left only tissue-associated persisters
337 (including some of the newly formed *S.*Tm 14028S Sm^R P2^{cat} cells) to survive (**Fig. 3A, Fig. 3-figure**
338 **supplement 1A**). We used ampicillin in the drinking water to suppress re-seeding of these tissue-
339 associated reservoirs before the third phase of the experiment. In this third phase, we introduced a
340 secondary recipient (SL1344 ΔP2) and monitored plasmid transfer (and thus the formation of
341 secondary transconjugants) to this strain. Strikingly, secondary transconjugants were formed in most
342 mice (3/5 mice, numbered 1-3; **Fig. 3A, Fig. 3-figure supplement 1A**; black dots), correlating with
343 both the presence of primary transconjugants in newly formed tissue reservoirs in the mLN, and re-
344 seeding of primary transconjugants (**Fig. 3B**; **Fig. Fig. 3-figure supplement 1B**). Importantly, *E. coli*
345 donors were not detected in this experiment after the ciprofloxacin treatment, suggesting that

346 plasmid transfer was due to re-seeding primary transconjugants from their new reservoirs (**Fig. 3-**
347 **figure supplement 1A-B**). We performed a series of control experiments to support that plasmid
348 transfer to secondary recipients was due to the re-seeding of primary transconjugants. In one control
349 experiment, we performed the same experiment as in **Fig. 3A-B** but modified the experiment in two
350 ways. First, we euthanized a subset of mice at day 15 (when we normally added the secondary
351 recipient) and determined that *E. coli* donors were not present in tissue reservoirs (**Fig. 3-figure**
352 **supplement 2**). Second, we tested to see if *E. coli* donors could survive antibiotic treatment generally
353 in the absence of *S.*Tm. We orally introduced donors in the absence of *S.*Tm and performed the same
354 antibiotic treatment regime as **Fig. 3A-B.** After the treatment regime, we added streptomycin to the
355 drinking water to select for any remaining *E. coli*. No *E. coli* could be detected, neither in the feces
356 nor in tissue reservoirs (**Fig. 3-figure supplement 3**). This confirmed that it is unlikely that *E. coli*
357 donors contributed to plasmid transfer after antibiotic treatment in **Fig. 3A-B**. Lastly, we performed a
358 different control experiment to investigate if plasmid transfer could in principle proceed within
359 tissues. This would address if invading secondary recipients could be receiving plasmids (within host
360 tissues) dependent on invasion into host tissues. We infected mice i.p. with both virulent *S.*Tm
361 donors (SL1344 P2^{cat}) and 5 minutes later with recipients (14028S). This sequential inoculation ruled
362 out conjugation in the inoculum. After 3 days, we examined the organs to quantify plasmid transfer.
363 While both donors and recipients were detected in the analyzed organs, transconjugants were not
364 detected, correlating with the absence of gut luminal growth (**Fig. 3-figure supplement 4)**.
365 Altogether, these data verified that primary transconjugants re-seeding into the gut lumen were
366 responsible for plasmid transfer to secondary recipients in **Fig. 3A**, and that plasmid transfer
367 preceded re-invasion into host tissues.
368 Next, we tested if multiple plasmids could accumulate in the gut lumen from tissue
369 reservoirs. We performed the first two phases of the experiment as above (**Fig. 3A-B**), but this time
370 in the third phase of the experiment, we added a second *E. coli* donor containing an extended-
371 spectrum beta-lactamase (ESBL) resistance plasmid (pESBL) shown to conjugate efficiently both in
372 antibiotic pre-treated mice and mice containing a reduced complexity microbiota (Bakkeren et al.,
373 2019; Benz et al., 2020). As in the previous experiment, P2^{cat} transconjugants were formed in the first
374 phase of the experiment, followed by the elimination of bacteria from the gut lumen and storage of
375 P2^{cat} transconjugants in tissue reservoirs in the second phase of the experiment (**Fig. 3C**; **Fig. 3-figure**
376 **supplement 1C-D**). Following the introduction of pESBL donors, pESBL transconjugants were
377 detected in most mice (4/7 mice) as additional recipients re-seeded from their reservoirs (**Fig. 3C;**
378 **Fig. 3-figure supplement 1C**). Importantly, in 2 of these 4 mice (labeled "a" and "b", P2^{cat}
379 transconjugants were also detected in the feces, suggesting that P2^{cat} transconjugants re-seeded
380 from their reservoirs (**Fig. 3C; Fig. 3-figure supplement 1C**). As in the other experiments, pESBL
381 transconjugants could also be detected in the mLN of one mouse (**Fig. 3D**). These data indicate that
382 invasive enteropathogens like *S.*Tm might allow different resistance plasmids to accumulate in tissue
383 reservoirs in the long run. However, it is important to reiterate that invasion into the mLN is likely
384 influenced by priority effects, making each subsequent invasion less likely. This may explain why both
385 types of transconjugants were not found in the same mLN in the tested mice (mouse "a" and "b"; **Fig.**
386 **3D**). Furthermore, while in this experiment both types of plasmids did not accumulate within the
387 same bacterial cell (likely because these are both *Inc*I1 plasmids and are therefore incompatible), it is
388 plausible that transconjugants containing multiple compatible plasmids could arise. Nevertheless, we
389 show that the accumulation of two plasmids in the gut lumen can be facilitated by tissue reservoirs.
390 Altogether, our data indicate that tissue reservoirs of *S.*Tm can influence plasmid spread in
391 the gut both by spreading plasmids to different recipients or accumulating multiple plasmids over
392 time.
393

394 **ESBL resistance plasmids can facilitate re-seeding of susceptible *S.*Tm recipients from tissue**
395 **reservoirs under beta-lactam treatment, and thereby promote resistance plasmid spread**
396
397 Our data suggest that some plasmids are selfish genetic elements that can use persistent
398 pathogen cells to form long term-reservoirs in host tissues. We reasoned that a subset of these
399 plasmids (e.g. those encoding for resistances that can clear antibiotics nearby, such as beta-
400 lactamases) may have another way to promote such transconjugant-dependent reservoir formation
401 by protecting potential recipients in their surroundings. The survival of *S.*Tm in the presence of
402 otherwise lethal concentrations of beta-lactam antibiotics mediated by ampicillin-resistant *E. coli* has
403 been described *in vitro*, based on the extracellular acting mechanism of beta-lactamases (Perlin et al.,
404 2009). Furthermore, antibiotic treatment is commonly used in the treatment of bacterial infections in
405 humans and livestock and beta-lactam antibiotics account for about 2/3 of the total antibiotic usage
406 worldwide (Cully, 2014; WHO, 2014, 2017). Therefore, we asked if gut luminal *Enterobacteriaceae*
407 harbouring plasmids that confer resistance to the antibiotic used could facilitate survival of *S.*Tm
408 recipients long enough to obtain a plasmid and survive in the gut lumen. As a class of multi-drug
409 resistance plasmids that has drawn particular attention as a contributor to antibiotic resistance
410 spread, and because of their extracellular mechanism of action, we chose to study ESBL plasmids
411 under beta-lactam treatment (Bajaj et al., 2016; Carattoli, 2009; Davies & Davies, 2010; WHO, 2017).
412 As previously, we infected *S.*Tm recipients (14028S Sm^R) i.p. into mice. One day post
413 infection, we introduced *E. coli* orally either bearing pESBL (same strains used in **Fig. 3C-D**; clinical
414 isolate characterized and sequenced in (Bakkeren et al., 2019; Benz et al., 2020)), or $P2^{cat}$ as a control
415 (isogenic *E coli* strains; the $P2^{cat}$ *E. coli* was cured of pESBL, followed by *in vitro* conjugation of $P2^{cat}$),
416 and simultaneously gave the mice ampicillin in the drinking water (**Fig. 4**). Treating mice with 0.5 g/L
417 ampicillin in the drinking water corresponds to a daily dose of 2-6g in a 70 kg human, close to the
418 recommended treatment schedule of oral ampicillin of 500mg every 6 hours (Wirfs, 2019). As
419 expected, *E. coli* pESBL grew to high densities, whereas in the control animals inoculated with
420 ampicillin susceptible *E. coli* $P2^{cat}$ (negative control donors; chloramphenicol resistance), the *E. coli*
421 could not survive (**Fig. 4-figure supplement 1A**). Over time, *S.*Tm began re-seeding from their tissue
422 reservoirs in both groups of mice (**Fig. 4-figure supplement 1B**), but could only bloom in the gut
423 lumen in the presence of pESBL *E. coli* (**Fig. 4A**). This bloom was associated with transfer of the
424 pESBL, followed by clonal expansion as *S.*Tm became resistant to ampicillin, leading to >99% of the
425 *S.*Tm gut luminal population obtaining a plasmid (**Fig. 4B**). Importantly, since *S.*Tm is an enteric
426 pathogen that utilizes inflammation to bloom in the gut (Stecher et al., 2007), using an ELISA for fecal
427 lipocalin-2, inflammation was detected in mice with pESBL *E. coli*, and reached particularly high levels
428 in mice where re-seeding of *S.*Tm occurred early during the experiment (i.e. $>10^3$ lipocalin-2 ng/g
429 feces; **Fig. 4C**). Interestingly, low-grade inflammation was detected in the absence of gut luminal
430 *S.*Tm (**Fig. 4C**) and could suggest that systemic *S.*Tm may contribute to low-grade gut inflammation,
431 propagated by gut luminal *E. coli*. To confirm that re-seeding of *S.*Tm was dependent on lowering the
432 concentration of fecal ampicillin by pESBL *E. coli*, we measured the concentration of fecal ampicillin
433 using mass spectrometry (**Fig. 4D**). In the presence of *E. coli* pESBL, fecal ampicillin concentrations
434 plummeted below the minimum inhibitory concentration (MIC; detected *in vitro* (Bakkeren et al.,
435 2019)) of *S.*Tm (**Fig. 4D**), likely explaining the re-seeding dynamics. Thus, donor mediated antibiotic
436 degradation may protect the re-seeding recipients and thereby promote pESBL transfer. Importantly,
437 as in the previous experiments, *S.*Tm transconjugants formed new plasmid reservoirs in host tissues,
438 primarily in the mLN (**Fig. 4E**). This indicates that ESBL plasmids promote their spread in host-
439 associated *Enterobacteriaceae* in two different ways: by lowering local antibiotic concentrations that
440 ensure survival of potential recipients, and by subverting tissue-lodged pathogens (persisters and
441 growing populations alike) to form long-term reservoirs within host tissues.
442

443 **Discussion:**
444
445 Our results suggest that plasmids can leverage facultative intracellular enteropathogenic
446 bacteria to promote both the formation of plasmid reservoirs in host tissues, and the spread of
447 plasmids into and among gut luminal microbes passing through a given host. In our experiments
448 using *S.*Tm infection in mice, repeated cycles of pathogen invasion and tissue reservoir formation
449 followed by re-seeding the gut lumen allow plasmids to form long-term reservoirs in the host's
450 tissues (**Fig. 5, steps 1-5**). These reservoirs act as a record of gut luminal horizontal gene transfer,
451 here shown by conjugation (**Fig. 1-4**). By assessing the genetic element's tissue reservoir formation,
452 our current study significantly extends the ecological implications of our previous work where we
453 had focused on persisters, showing that these antibiotic persisters can promote the release of donors
454 into the gut lumen (Bakkeren et al., 2019). Here we show that tissue reservoirs can influence plasmid
455 dynamics also without selection for persister survival in antibiotic treated tissues (**Fig. 5, step 1**).
456 Most likely, tissue reservoir-promoted plasmid transfer dynamics will likely happen during persistent
457 infection involving phenotypically susceptible pathogen cells, provided multiple strains co-occur
458 within a host. Since a natural ecological succession of *Enterobacteriaceae* has been documented in
459 the gut (Leon-Sampedro et al., 2021; Martinson et al., 2019), an overarching re-seeding-conjugation-
460 reinvasion cycle could result in the distribution of different alleles in the various strains colonizing a
461 host. The host tissue reservoirs would dramatically expand the time scale of such transfer thereby
462 enabling horizontal gene transfer even when the initial donor and the later recipient have never "co-
463 existed" within the host. Such co-existence-independent gene exchange could pertain to resistance
464 genes or virulence determinants alike. In line with this hypothesis, different strains of commensal
465 and pathogenic *Enterobacteriaceae* that show vastly different plasmid, prophage and mutational
466 profiles are often observed within a given host population or even within the same host (Desai et al.,
467 2013; Kroger et al., 2012; Martinson et al., 2019; San Roman et al., 2018; Tenaillon et al., 2010).
468 Conversely, the same plasmid has been detected in different enterobacterial strains over time within
469 the same patient (Leon-Sampedro et al., 2021). The role of the pathogen's re-seeding-acquisition-
470 reinvasion cycles in resistance plasmid transfer may be particularly important in cases where
471 different *S.*Tm are present within the same host (e.g. the gut lumen vs. the host tissues), as observed
472 in pig farms (San Roman et al., 2018).
473 Which factors limit plasmid storage and transfer from host-tissue reservoirs? Through
474 population dynamic analysis, we showed that re-seeding of recipient strains from tissue reservoirs is
475 the rate-limiting step for the formation of new transconjugant reservoirs (**Fig. 2; Fig. 5, step 2a**). This
476 is in line with our previous work (Bakkeren et al., 2019) where we suggested that donor-re-seeding
477 from persister reservoirs in host tissues is a rate limiting process, and reinforces the importance of
478 understanding the mechanisms of re-seeding, host tissue invasion and the formation of new tissue
479 reservoirs. Previous studies have suggested the gall bladder as a route of re-seeding for *Salmonella*
480 via bile secretions (Everest et al., 2001; Gonzalez-Escobedo et al., 2011; Lam & Monack, 2014). In our
481 experimental model, we found that sequence tags in the gall bladder did not necessarily correlate
482 with those found at highest density in the feces, suggesting, along with others (Lam & Monack,
483 2014), that additional routes of re-seeding may exist. Phagocytic cells such as macrophages and
484 dendritic cells serve as reservoirs for *S.*Tm (Claudi et al., 2014; Helaine et al., 2014; Kaiser et al., 2014;
485 Pham et al., 2020; Rosenberg et al., 2021; Stapels et al., 2018) and can be reactivated by IFNγ
486 depletion (Monack et al., 2004). The high density of *S.*Tm in the tissues that line the small intestine
487 including the gut associated lymphoid tissues (here called S.I. GALT), correlating with *S.*Tm found in
488 the gut lumen of the small intestine, could suggest that trafficking of *S.*Tm-bearing immune cells to
489 these sites (Habtezion et al., 2016) contributes to gut luminal re-seeding. The independence of *S.*Tm
490 on its TTSS-1 for re-seeding appears to support host-mediated trafficking to the gut lumen rather
491 than an active mechanism evolved by *S.*Tm, but further work is needed for confirmation.

492 Interventions such as vaccination have shown success in reducing the formation of tissue
493 reservoirs and consequently plasmid transfer dynamics associated with re-seeding (Bakkeren et al.,
494 2019; Moor et al., 2017; Moor et al., 2016). Here, we showed that once re-seeding occurred, the
495 transfer of plasmids followed by reinvasion is likely, given a sufficiently high carrying capacity (as a
496 proxy for decreased colonization resistance) in the gut lumen. This is because plasmid transfer is
497 dependent on both the density of donors and recipients. Invasion may also be density dependent
498 (Ackermann et al., 2008); approximately 300 invasion events occur into the mLN per day initially in
499 streptomycin pretreated mouse models (Kaiser et al., 2013) and this likely decreases proportionally
500 with colonization. In a healthy microbiota community, colonization resistance prohibits
501 enterobacteriaceal blooms in >90% of the hosts (Stecher et al., 2010; Stecher & Hardt, 2011) and
502 dramatically reduces the efficiency of plasmid transfer (Stecher et al., 2012; Wotzka et al., 2019).
503 However, gut perturbations such as diet shifts, inflammation, antibiotic treatment, or a reduction in
504 microbiota complexity (e.g. dysbiosis) can all lead to increases in loads of *Enterobacteriaceae* and
505 consequently plasmid transfer (**Fig. 5, step 3)** (Bakkeren et al., 2019; Barthel et al., 2003; Benz et al.,
506 2020; Kreuzer & Hardt, 2020; Stecher et al., 2012; Stecher et al., 2007; Wotzka et al., 2019).
507 Therefore, a healthy microbiota is integral in minimizing pathogen evolution in two complementary
508 ways, by reducing horizontal gene transfer and by reducing the likelihood of re-invasion and
509 subsequent formation of tissue reservoirs. Further work will be needed to validate how such
510 perturbations accelerate the dynamics of plasmid spread and reservoir formation.
511 Lastly, we showed that plasmids encoding secreted antibiotic degrading enzymes can
512 promote their own spread by an additional mechanism *in vivo*: protecting potential new recipients
513 sensitive to the antibiotic (**Fig. 5, step 2b**). Re-seeding of *S.*Tm, initially susceptible to the beta-
514 lactam, can occur even during beta-lactam therapy, dependent on the presence of *E. coli* producing
515 beta-lactamase (**Fig. 4**). The prevalence of ESBL-producing *E. coli* is rising in recent years, and ESBL
516 genes are frequently plasmid-encoded (Temkin et al., 2014; WHO, 2017; Yang et al., 2009). The
517 extracellularly acting beta-lactamases are therefore public goods. *In vitro* this was shown to allow the
518 survival of susceptible *S.*Tm in the presence of otherwise lethal concentrations of ampicillin (Perlin et
519 al., 2009). In our experiments, we showed that the same process occurs in the gut lumen, with re-
520 seeding *S.*Tm followed by conjugation, clonal expansion, and tissue reinvasion as a consequence (**Fig.
521 4**). As one of the prodigal mechanisms for blooms (of resistant bacteria), antibiotic treatment could
522 serve to amplify re-seeding followed by plasmid exchange and tissue reservoir reformation, given
523 sufficient protection from the antibiotic *in trans.* This obviously depends on the presence of tissue-
524 invasive enteropathogens in the hosts, which is quite common in today's farming industry (San
525 Roman et al., 2018; Van Boeckel et al., 2019), as well as the mechanism of action of the antibiotic
526 used. Many antibiotic resistance genes encode antibiotic-inactivating enzymes, even if they are not
527 secreted (D'Costa et al., 2006), as is the case of beta-lactamases. However, it remains to be seen to
528 what extent non-secreted inactivating enzymes can deplete local concentrations of the antibiotic *in
529 vivo*. Conversely, pathogen intrinsic mechanisms transiently promoting survival may further prolong
530 recipient survival in an antibiotic loaded gut lumen and thereby further promote plasmid spread. The
531 transient overexpression of efflux pumps was shown to confer survival long enough to obtain a
532 plasmid in the presence of tetracycline above the MIC *in vitro* (Nolivos et al., 2019). Moreover,
533 bacterial strains that produce outer membrane vesicles have been shown to lead to an altered
534 susceptibility to antimicrobial peptides (e.g. polymyxin B or colistin, shown in several bacteria
535 including *E. coli* and *Salmonella* Typhi) (Manning & Kuehn, 2011; Marchant et al., 2021). One study
536 found that polymyxin resistance could even be functionally transferred to sensitive bacteria
537 mediated by outer membrane vesicles (Marchant et al., 2021). It is therefore plausible that
538 mechanisms aside from secreted and diffusible enzymes (such as for beta-lactamases) could
539 contribute to re-seeding and plasmid acquisition. However, further work will be necessary to

540 determine different possible mechanisms for cross-protection of susceptible strains by resistant cells
541 in the gut lumen.
542 Overall, here we show that plasmids can subvert tissue-associated pathogen reservoirs to
543 promote long-term carriage within the host and subsequent spread. There seem to be two types of
544 tissue reservoirs with partially complementary features (**Fig. 5**). The tissue-associated reservoirs
545 formed by enteropathogens in chronic (persistent) infections are relatively large and facilitate re-
546 seeding of the gut lumen and subsequent plasmid transfer at relatively high rates. In contrast,
547 persistent pathogen cells are less frequent and need to re-start growth before engaging in any
548 luminal plasmid transfers, likely making them less efficient at luminal re-seeding. However, they
549 ensure survival of recipients and plasmid reservoir maintenance even in cases of therapy with
550 antibiotics to which these persisters are genetically susceptible. Although in our experimental model
551 plasmids can benefit strongly from tissue reservoirs, their actual transfer is dependent on the strain
552 densities in the gut lumen. Our study provides a proof-of-concept that tissue reservoirs can act as a
553 record of evolutionary events such as plasmid transfer in the gut lumen. It is conceivable that
554 mutational events or transfer of other mobile genetic elements, for example bacteriophages carrying
555 accessory genes, could also be stored in tissue reservoirs. Regardless, it remains to be seen how
556 often such cases occur in nature, since our work identifies these processes to be dependent on the
557 carrying capacity in the gut and conjugation rates of plasmid-strain pairs, and to what extent this
558 contributes to the dissemination of accessory genes on mobile genetic elements, such as antibiotic
559 resistance genes.

560 **Figure captions:**
561
562 **Figure 1. *S.*Tm in tissue reservoirs can re-seed the gut lumen, obtain a plasmid from**
563 **Enterobacteriaceae in the gut lumen, and form new plasmid-bearing reservoirs. A)** Proposed
564 hypothesis. *S.*Tm recipients (green) establish tissue reservoirs after intraperitoneal injections and
565 spread to organs, dependent on the Type-three secretions system-2 (TTSS-2; encoded on SPI-2). The
566 microbiota (grey) provides colonization resistance against colonization of the gut lumen. Donors
567 (blue) colonize the gut lumen by an oral infection following a streptomycin treatment to suppress the
568 microbiota. *S.*Tm recipients re-seed from their reservoirs and obtain a plasmid from donors forming a
569 transconjugant (red). These transconjugants then form new tissue reservoirs. **B)** Transconjugants are
570 formed in the gut lumen. Mice were i.p. infected with 10^3 CFU of a 1:1:1 mix of 14028S Sm^R *TAG1-3*
571 ($S.Tm^{WT}$; n=13) or 10^3 CFU of $14028S^{SPI-2}$ SmR ($S.Tm^{SPI-2}$; *ssaV* mutant; n=8). On day 2 post infection,
572 20 mg of streptomycin was given 4 hours before $5x10^7$ CFU of a 1:1:1:1 mix of $S.Tm^{Avir}$ (*invG ssaV*
573 mutant) $P2^{TAG4-7}$. Selective plating was used to determine the fecal transconjugant loads. **C)** Tissue
574 reservoirs of *S.*Tm. Organs of mice in **panel B** were analyzed for recipients (green circles) or
575 transconjugants (red circles). **B-C)** Dotted line indicates the detection limit. A two-tailed Mann
576 Whitney-U test was used to compare $S.Tm^{WT}$ (solid circles) to $S.Tm^{SPI-2}$ (hollow circles) in each sample
577 ($p>0.05$ not significant (ns), $p<0.05$ (*), $p<0.01$ (**), $p<0.001$ (***), $p<0.0001$ (****)). **D)** *S.*Tm
578 recipients can obtain $P2^{cat}$ from *E. coli*. Mice were i.p. infected with 10^3 CFU of 14028S Sm^R *TAG1*
579 ($S.Tm^{WT}$; n=12). On day 2 post infection, 20 mg of streptomycin was given 4 hours before $5x10^7$ CFU
580 of *E. coli* 536 $P2^{cat}$. Selective plating and colony colour on MacConkey agar was used to determine the
581 fecal transconjugant loads. **E**) Tissue reservoirs of *S.*Tm after conjugation with *E. coli*. Organs in **panel**
582 **B** were analyzed for recipients (green squares) or transconjugants (red squares). **D-E)** Dotted line
583 indicates the detection limit. **B,D)** Bars indicate median. **C,E)** Lines indicate median. GB = gall bladder;
584 mLN = mesenteric lymph node. **B-E)** Fecal populations of donors, recipients, and transconjugants are
585 presented in **Fig. 1-figure supplement 1**.
586
587 **Figure 2. Re-seeding from tissue reservoirs is a rate limiting step that suffices in conjugation and**
588 **formation of new reservoirs given a sufficient carrying capacity. A-B)** Mice in **Fig. 1** where re-
589 seeding of recipients occurred (n=10) were analyzed for the distribution of sequence tags in
590 enrichments of recipients at day 10 of the experiment (including transconjugants) by qPCR (raw tag
591 data shown in **Fig. 2-figure supplement 1**). The dotted line indicates the conservative detection limit.
592 Lines indicate the median. The proportions of tags are plotted relative to all 7 tags (3 recipient and 4
593 plasmid tags). **A)** Recipient tags and **B)** plasmid tags were sorted according the most abundant
594 recipient or plasmid tag in the feces, in each mouse. GB = gall bladder; mLN = mesenteric lymph
595 node. **C)** Fitting of simulations to experimental data. Individual summary statistics used to fit
596 simulations are shown in **Fig. 2-figure supplement 3**. Parameters and method for fitting is described
597 in **Supplementary information.** The migration rate of $\mu=1.78$ recipient CFU/g feces per day and the
598 conjugation rate of $\gamma=3.16x10^{-11}$ events per CFU/g feces per day provide the best fit to the
599 experimental data (red indicates rate pairs that fit the experimental data most often). **D)** The
600 migration and conjugation rates were fixed to the most likely values in **panel C** and the carrying
601 capacity was varied. Recipient (green) and transconjugant (red) populations at the end of the
602 simulation (day 10; n=100 simulations per carrying capacity) are shown as the mean with the range
603 of values. The lowest value was set to 1 CFU/g feces to allow visualization on a log scale. The grey
604 dotted lines correspond to the carrying capacity at which transconjugants are present at 10^6 CFU/g
605 feces, as a density threshold that we speculate should facilitate some frequency of invasion into
606 tissue reservoirs.
607

608 **Figure 3. Newly formed plasmid reservoirs can spread plasmids to recipients after antibiotic**
609 **treatment and plasmids can accumulate in the gut dependent on tissue reservoirs. A)** *S.*Tm
610 transconjugants can conjugate to secondary recipients after survival of antibiotic treatment, by
611 survival in tissue reservoirs. Mice were i.p. infected with 10^3 CFU of 14028S Sm^R *TAG1* (Kan^R; n=5). On
612 day 2 post infection, 20 mg of streptomycin was given 4 hours before $5x10^7$ CFU of *E. coli* 536 $P2^{cat}$
613 (CmR). Selective plating and colony colour on MacConkey agar was used to determine the fecal
614 transconjugant loads (red circles). On day 10, mice were given 3 mg ciprofloxacin for three days in a
615 row, along with 2 g/l ampicillin in the drinking water from day 11-15. On day 15, a secondary
616 recipient (SL1344 ΔP2; Amp^R) was added ($5x10^7$ CFU oral). Selective plating allowed the enumeration
617 of secondary transconjugants (black circles). Bars indicate the median. Dashed black lines connect
618 primary or secondary transconjugant populations of the same mice (mice are numbered 1-3; the
619 same numbering is used in **panel B**). **B)** Tissue reservoirs of *S.*Tm. Organs of mice in **panel A** were
620 analyzed for primary transconjugants and secondary transconjugants. Lines indicate the median. GB
621 = gall bladder; mLN = mesenteric lymph node. The numbers correspond to the same mouse
622 numbering as in **panel A**. **C)** *S.*Tm recipients can allow the formation of multiple transconjugants over
623 time dependent on multiple re-seeding events. Mice (n=7) were i.p. infected with recipients 14028S
624 Sm^R *TAG1* (Kan^R) and donors *E. coli* 536 $P2^{cat}$ (CmR) as in **panel A**. On day 10, mice were given
625 antibiotics as in **panel A**. On day 15, a second donor, (*E. coli* pESBL; Amp^R) was added ($5x10^7$ CFU
626 oral). Selective plating allowed the enumeration of both $P2^{cat}$ (red squares) and pESBL
627 transconjugants (grey squares). Bars indicate the median. **D)** Tissue reservoirs of *S.*Tm. Organs of
628 mice in **panel C** were analyzed for $P2^{cat}$ and pESBL transconjugants. Lines indicate the median. GB =
629 gall bladder; mLN = mesenteric lymph node. Dashed lines connect the two transconjugant
630 populations in the same fecal sample (two mice harbor both types of transconjugants: mouse (a) and
631 (b); these mouse labels are also shown on the mLN population). **A-D)** Dotted lines indicate the
632 detection limits. Population sizes of all strains and subpopulations are presented in **Fig. 3-figure**
633 **supplement 1**.
634
635 **Figure 4. Re-seeding of *S.*Tm followed by reception of a plasmid and storage in new tissue**
636 **reservoirs can occur under beta-lactam counter-selection, dependent on *E. coli* conjugative ESBL**
637 **plasmids. A-E)** Mice were i.p. infected with 10^3 CFU of a 1:1:1:1:1:1:1 mix of 14028S Sm^R *TAG1-7*
638 (Kan^R). On day 1 post infection, mice were given 0.5 g/l ampicillin in the drinking water and either
639 $5x10^7$ CFU of *E. coli* $P2^{cat}$ (Cm^R; black circles; n=10) or *E. coli* pESBL (Amp^R; orange circles; n=10).
640 Dotted lines indicate detection limits. Lines connect medians on each day. A two-tailed Mann
641 Whitney-U test was used to compare $S.Tm^{WT}$ + *E. coli* $P2^{cat}$ to $S.Tm^{WT}$ + *E. coli* $P2^{cat}$ in each sample
642 ($p>0.05$ not significant (ns), $p<0.05$ (*), $p<0.01$ (**), $p<0.001$ (***), $p<0.0001$ (****)). **A)** Re-seeding
643 *S.*Tm was analyzed by selective plating on kanamycin-containing MacConkey agar. **B)** Conjugation
644 was determined by selective and/or replica plating. The proportion transconjugants is calculated by
645 the population size of transconjugants divided by the sum of both transconjugants and recipients.
646 The grey dashed line indicates a proportion of 1. The dotted line indicates the conservative detection
647 limit for transconjugants (since the proportion depends on the recipient population size, each sample
648 has a different detection limit and therefore values can appear below the detection limit. Values in
649 the grey box in the lower part of the y-axis are plotted to indicate mice with no re-seeding. **C)**
650 Inflammation was quantified using an ELISA for fecal lipocalin-2. **D)** Fecal ampicillin was measured
651 using mass spectrometry. The blue dashed line indicates the minimum inhibitory concentration of
652 *S.*Tm *in vitro* (Bakkeren et al., 2019). The red dashed line indicates the concentration of ampicillin
653 given to the mice in the drinking water. **E)** Organs were analyzed for transconjugant populations on
654 day 10 of the experiment. GB = gall bladder; mLN = mesenteric lymph node.
655

656 **Figure 5. Working model for how the infection cycle of *S.*Tm may promote the spread and**
657 **accumulation of plasmids within a host.** Invasive *S.*Tm (green for recipients, red for transconjugants)
658 can establish reservoirs within host tissues, storing their current plasmid complement in these
659 reservoirs (n plasmids). A sub-population of these cells can survive antibiotic treatment as persisters
660 (smaller green or red cells), that can regrow after the withdrawal of antibiotics. In extension to
661 previous work (Bakkeren et al., 2019), here we show that reservoirs of *S.*Tm that chronically infect
662 the host can re-seed from host tissues, even in the absence of selection for persisters (**step 1**). Exiting
663 the host tissues into the gut lumen is a rate-limiting process (**step 2a**; (Bakkeren et al., 2019)). This
664 process can be facilitated by Enterobacteriaceae donors (blue; plasmid shown in black) that produce
665 extracellularly acting plasmid-encoded antibiotic resistance genes (such as beta-lactamases; blue
666 colour radiating from the cell indicates local degradation of beta-lactam antibiotics by beta-
667 lactamases), that can allow the local survival of re-seeding recipients under antibiotic treatment
668 (**step 2b**). Once both donors and recipients co-occur in the gut lumen at sufficient density, plasmid
669 transfer proceeds (**step 3**; (Bakkeren et al., 2019; Benz et al., 2020; Diard et al., 2017; Moor et al.,
670 2017; Stecher et al., 2012; Wotzka et al., 2019)). When colonization resistance is relaxed, invasive
671 transconjugants (red) can reach sufficient densities to invade back into host tissues and form new
672 reservoirs that now contain n+1 plasmids (**step 4**). In the tissue, transconjugant subpopulations can
673 also survive antibiotic therapy as persisters (smaller red cells). This process is repeatable in certain
674 conditions. Either transconjugants can re-seed to donate the plasmid to further gut luminal
675 recipients (**step 5a**), or recipients can re-seed to receive an additional plasmids (**step 5b**). Novel steps
676 of this process, demonstrated here using the streptomycin treatment mouse model, are indicated
677 with bold numbers, whereas steps that have been previously shown are indicated with non-bold
678 numbers (and key references are listed in the caption).
679
680

681 **Materials and methods:**

682

683 **Strains, plasmids, and primers used in this study**

684

685 Bacterial strains used in this study are derivatives of *S.*Tm SL1344 (Hoiseth & Stocker, 1981),
686 *S.*Tm ATCC 14028S (Jarvik et al., 2010), *E. coli* 536 (Berger et al., 1982; Brzuszkiewicz et al., 2006), or
687 *E. coli* ESBL15 (Bakkeren et al., 2019; Tschudin-Sutter et al., 2016), and are listed in **Table 1**. For
688 cultivation of bacterial strains, lysogeny broth (LB) medium was used containing the appropriate
689 antibiotics (50 µg/ml streptomycin (AppliChem); 50 µg/ml kanamycin (AppliChem); 15 µg/ml
690 chloramphenicol (AppliChem); 100 µg/ml ampicillin (AppliChem)) at 37°C (or 30°C if containing pCP20
691 or pCP20-IncI1). Genetic constructs (e.g. gene deletions, neutral isogenic sequence tags, or the P3
692 plasmid) were introduced into the desired background strain using P22 HT105/1 *int-201* phage
693 transduction (Sternberg & Maurer, 1991). Bacterial plasmids used to confer resistance or for
694 construction of strains are listed in **Table 2** and were transformed into cells using electroporation.
695 *E. coli* ESBL 15 was cured of its plasmid, pESBL, using plasmid incompatibility. To create an
696 incompatible plasmid, pCP20-IncI1 was cloned using the replicon of pESBL. A PCR amplicon of the
697 replication initiation protein of pESBL with 831 and 420 bp upstream and downstream flanking
698 regions, respectively (to ensure the entire replicon was cloned), was cloned into pCP20 digested with
699 *Pst*I and *Eco*RV (removing the ampicillin resistance cassette) using Gibson Assembly (NEB; protocol as
700 described by the manufacturer). The resulting plasmid, pCP20-IncI1, was electroporated into *E. coli*
701 ESBL15 and grown at 30°C under chloramphenicol selection. Loss of resistance of ampicillin (and
702 consequently loss of pESBL) was confirmed by streaking on LB with ampicillin. The resulting clones
703 were restreaked on LB without chloramphenicol grown at 37°C to cure pCP20-IncI1.
704 Conjugative plasmids were transferred into the desired strain (e.g. P2^{cat} into *E. coli* ΔpESBL
705 and *E. coli* 536) using *in vitro* conjugation assays. In brief, 10^5 CFU from an overnight culture of the
706 donor strain (SL1344 P2^{cat}) was mixed with the desired recipient, allowing conjugation overnight at
707 37°C on a rotating wheel. Cells were plated on selective MacConkey agar to identify transconjugants
708 by resistance phenotype and/or colour (i.e., *S.*Tm is *lac* negative and thus forms yellow colonies on
709 MacConkey agar while *E. coli* is *lac* positive and forms red colonies).
710 All strains and plasmids were genotyped prior to use using the primers listed in **Table 3**.

711

712 **Table 1. Strains used in this study**

Strain name	Strain Number	Relevant genotype	Resistance*	Reference
SL1344	SB300	Wild-type	Sm	(Hoiseth & Stocker, 1981)
ATCC 14028S	14028S	Wild-type	None	(Jarvik et al., 2010)
SL1344 P2^{cat}	M995	*cat* on P2	Sm, Cm	(Stecher et al., 2012)
SL1344 ΔP2	M1404	P2 cured	Sm	(Stecher et al., 2012)
E. coli 536	Z2366	Wild-type	Sm	(Berger et al., 1982; Brzuszkiewicz et al., 2006)
E. coli 536 P2^{cat}	Z2124	*cat* on P2	Sm, Cm	This study
SL1344 ΔP2 pM975	Z2287	P2 cured; *bla*	Sm, Amp	This study
E. coli ESBL15	Z2115	*CTX-M1 on pESBL*	Amp	(Bakkeren et al., 2019; Tschudin-

				Sutter et al., 2016)
14028S Sm^R	T186	*strAB* on P3	Sm	This study
14028S Sm^R *TAG1*	Z2279	*WITS1-aphT*	Sm, Kan	This study
14028S Sm^R *TAG2*	Z2281	*WITS2-aphT*	Sm, Kan	This study
14028S Sm^R *TAG3*	Z2283	*WITS11-aphT*	Sm, Kan	This study
14028S Sm^R *TAG4*	T270	*WITS13-aphT*	Sm, Kan	This study
14028S Sm^R *TAG5*	T272	*WITS17-aphT*	Sm, Kan	This study
14028S Sm^R *TAG6*	T274	*WITS19-aphT*	Sm, Kan	This study
14028S Sm^R *TAG7*	T276	*WITS21-aphT*	Sm, Kan	This study
14028S^{SPI-2} Sm^R	T284	*ssaV::aphT*	Sm, Kan	This study
SL1344^{Avir} $P2^{TAG4}$	Z2292	*WITS13-cat* on P2; Δ*invG* Δ*ssaV*	Sm, Cm	This study
SL1344^{Avir} $P2^{TAG5}$	Z2293	*WITS17-cat* on P2; Δ*invG* Δ*ssaV*	Sm, Cm	This study
SL1344^{Avir} $P2^{TAG6}$	Z2294	*WITS19-cat* on P2; Δ*invG* Δ*ssaV*	Sm, Cm	This study
SL1344^{Avir} $P2^{TAG7}$	Z2295	*WITS21-cat* on P2; Δ*invG* Δ*ssaV*	Sm, Cm	This study
E. coli ΔpESBL	Z2156	pESBL cured	None	This study
E. coli ΔpESBL $P2^{cat}$	T305	pESBL cured; *cat* on P2	Cm	This study
14028S^{SPI-1} Sm^R	T2429	*invG::aphT*	Sm, Kan	This study

* Relevant resistances only: Sm = ≥50 µg/ml streptomycin; Cm = ≥15 µg/ml chloramphenicol; Kan = ≥50 µg/ml kanamycin; Amp = ≥100 µg/ml ampicillin.

Table 2. Plasmids used in this study

Plasmid name	Relevant genotype	Resistance	Reference
pM975	*bla*; used to confer ampicillin resistance	Amp	(Hapfelmeier et al., 2005)
pCP20	FLP recombinase	Amp, Cm	(Datsenko & Wanner, 2000)
pCP20-IncI1 (pZ2496)	FLP-*bla*::*IncI*1 replicon	Cm	This study
P3 (pRSF1010)	*strAB*	Sm	(Kroger et al., 2012)
P2 (pCol1b9)	Wild-type	None	(Stecher et al., 2012)
$P2^{cat}$	*cat*	Cm	(Stecher et al., 2012)
$P2^{TAG}$	*WITS13, 17, 19,or 21-cat* on P2	Cm	(Bakkeren et al., 2019)
pESBL (pESBL15)	*CTX-M-1*	Amp	(Bakkeren et al., 2019; Tschudin-Sutter et al., 2016)

Table 3. Primers used in this study

Primer name	Sequence (5' to 3')	Purpose	Reference
ESBL15_repl_gibs_for	GCC AGT TAA TAG TTT GCG CAA CGT TGT TGC CAT TGC TGC ACT GAG CTA CCA TAG ATG AC	PCR amplification of *IncI*1 replicon from pEBSL for Gibson assembly	This study
ESBL15_repl_gibs_rev	TAC AAT TAT TCC TTA CTA TGG ACA AAA ACA TCA ATC TGA T GTG GTT TCA GAA CGG TGA G	PCR amplification of *IncI*1 replicon from pEBSL for Gibson assembly	This study
ESBL15_ori_ver_up	CCA GTT AAT AGT TTG CGC AAC	Validation of pCP20-IncI1 cloning	This study
ESBL15_ori_intl_ rev	CTT TCA GCG CTT TAT AGC G	Validation of pCP20-IncI1 cloning	This study

ESBL15_ori_intl_for	CTG TTC CGA TGA CCA TCT G	Validation of pCP20-IncI1 cloning	This study
ESBL15_ori_ver_dw	CTC CAG TTT AAA TAC AAG ACG	Validation of pCP20-IncI1 cloning	This study
ssaV-137F	GCAGCGTTCCAGGGTATTCC	Verification of Δ*ssaV* in the chromosome	(Bakkeren et al., 2021)
ssaV+155R	CAGCAAGTTCTTCTCCAGGC	Verification of Δ*ssaV* in the chromosome	(Bakkeren et al., 2021)
invG-134F	GAAGGCCACGAGAACATCAC	Verification of Δ*invG* in the chromosome	(Bakkeren et al., 2021)
invG+112R	GCGGCCTGTTGTATTTCCGC	Verification of Δ*invG* in the chromosome	(Bakkeren et al., 2021)
P3_SmR_for	CTA GTA TGA CGT CTG TCG C	Verification of P3	This study
P3_SmR_rev	CAC GTT TCG CAA CCT GTT C	Verification of P3	This study
WITS1	ACG ACA CCA CTC CAC ACC TA	qPCR for TAG1	(Grant et al., 2008)
WITS2	ACC CGC AAT ACC AAC AAC TC	qPCR for TAG2	(Grant et al., 2008)
WITS11	ATC CCA CAC ACT CGA TCT CA	qPCR for TAG11	(Grant et al., 2008)
WITS13	GCT AAA GAC ACC CCT CAC TCA	qPCR for TAG13	(Grant et al., 2008)
WITS17	TCA CCA GCC CAC CCC CTC A	qPCR for TAG17	(Grant et al., 2008)
WITS19	GCA CTA TCC AGC CCC ATA AC	qPCR for TAG19	(Grant et al., 2008)
WITS21	ACA ACC ACC GAT CAC TCT CC	qPCR for TAG21	(Grant et al., 2008)
ydgA	GGC TGT CCG CAA TGG GTC	qPCR for all tags	(Grant et al., 2008)
pagJ_fwd	ATC TTC GGG GAA GGG CAC GTC CG	14028S chromosome-specific PCR	This study
pagJ_rev	GCT GTA ACC GTA AGG ATA GTG TGC CAC AAT T	14028S chromosome-specific PCR	This study
cat_fwd	GCATTTCAGTCAGTTGCTCAATGTACCT ATAACC	$P2^{cat}$-specific PCR	This study
cat_rev	CGACATGGAAGCCATCACAAACGG	$P2^{cat}$-specific PCR	This study

Infection experiments

All animal experiments were performed in 8-12 week-old specified opportunistic pathogen-free (SOPF) 129/SvEv mice. These mice contain a functional *Nramp1* allele (also known as *Slc11a1*) and are resistant to *S.*Tm and therefore allow for long-term infections (Cunrath & Bumann, 2019; Stecher et al., 2006). All infection experiments were approved by the responsible authorities (Tierversuchskommission, Kantonales Veterinäramt Zürich, licenses 193/2016 and 158/2019). Sample size was not predetermined and mice were randomly assigned to treatment groups.

For all experiments, overnight cultures of recipient *S.*Tm (14028S Sm^R derivatives) containing the appropriate antibiotics were washed with sterile PBS 2x before being diluted to 10^4 CFU/ml in PBS. Mixtures of the appropriate strains (in the case of tagged strains) or single strains were intraperitoneally injected into mice as a 100 µl volume (~10^3 CFU per mouse). All mice used for plasmid transfer experiments were housed in individual cages to ensure experimental independence. For experiments that lasted longer than 10 days, mice were caged in pairs initially, but split to individual cages for the final 10 days (due to ethical reasons, mice were not individually caged for longer than 10 days).

On day 2 post infection, mice were given an oral dose of streptomycin (20 mg), as previously described for the streptomycin pretreated mouse model (Barthel et al., 2003). Overnight cultures of

739 donor strains (Sm^R; SL1344 or *E. coli* 536 derivatives) containing the appropriate antibiotics were
740 subcultured for 4 hours 1:20 in 2 ml LB without antibiotics, and then washed in PBS. 4 hours after
741 streptomycin treatment, donors were given orally (~$5x10^7$ CFU per mouse). After 10 days, mice were
742 either euthanized or given doses of oral ciprofloxacin (3 mg per mouse; ciprofloxacin hydrochloride
743 monohydrate, Sigma-Aldrich, dissolved in 100 µl sterile dH_2O) for three consecutive days, while
744 ampicillin (2 g/L) was provided in the drinking water on days 11-15 to prevent re-seeding before the
745 third strain was added. After each ciprofloxacin treatment, cages were changed to prevent
746 reinfection due to coprophagy. On day 15 of the experiment, mice were either euthanized, or given a
747 third strain (either a second recipient or a second donor; Amp^R). These mice were euthanized on day
748 22. For **Fig. 3-figure supplement 3**, mice were not i.p. infected with 14028S, so the experiment
749 started with an oral streptomycin treatment (20mg) 4 hours prior to infection with *E. coli* 536 $P2^{cat}$.
750 The rest of the experiment was treated the same as **Fig. 3**, but after 4 days of ampicillin in the
751 drinking water (as above), the mice were switched to streptomycin drinking water (1 g/L) for 3 days
752 before euthanasia.
753 For mice used to enrich for persisters in tissue reservoirs (**Fig. 1-figure supplement 5**),
754 ceftriaxone (1.5 mg ceftriaxone disodium salt hemi(heptahydrate) dissolved in 100 µl PBS; Sigma-
755 Aldrich) was injected intraperitoneally for 3 consecutive days. Donors were added after a
756 streptomycin treatment (as above) on day 6 and again without streptomycin on day 8 to ensure
757 robust colonization. These mice were euthanized on day 15.
758 For mice used to analyze plasmid transfer within tissues (**Fig. 3-figure supplement 4)**,
759 overnight cultures of SL1344 $P2^{cat}$ and 14028S Sm^R Kan^R were washed with sterile PBS 3x before
760 being diluted to 10^4 CFU/ml in PBS. 50 µl of each strain was injected into the same side of the mouse
761 by an i.p. injection, 5 minutes sequentially (total CFU ~10^3 CFU per mouse). Mice were kept for 3 days
762 before euthanasia and analysis of organs.
763 For mice used to investigate re-seeding in the presence of ampicillin counterselection
764 dependent on ESBL-producing *E. coli* (**Fig. 4**), on day 1 post intraperitoneal infection of recipients, the
765 mice were given 0.5 g/L ampicillin in the drinking water and given ~$5x10^7$ CFU pESBL or $P2^{cat}$ *E. coli*
766 donors orally (in PBS, following a 4 hours subculture as described above). An ELISA for mouse
767 lipocalin-2 was performed on feces (protocol according to the manufacturer; R&D Systems kit) to
768 determine the inflammatory state of the gut.
769 In all mouse experiments, feces were collected daily into pre-weighed Eppendorf tubes and
770 homogenized in PBS using a steel ball at 25 Hz for 1 minute. Populations of donors, recipients, and
771 transconjugants were diluted and enumerated using selective MacConkey agar. Replica plating was
772 used to accurately determine the ratio of recipients or donors to transconjugants if transconjugants
773 were on the same order of magnitude as the donors or recipients. When mice were euthanized (at
774 day 2, 10, 15, or 22; specified in the figure legends), the spleen, liver, gall bladder, and mesenteric
775 lymph node, were collected and homogenized in PBS. Populations of bacteria were enumerated as
776 for the feces. For mice euthanized at day 2 post infection (**Fig. 1-figure supplement 6**), additional
777 organs were collected. For the duodenum, jejunum, ileum, cecum, and colon, first the content was
778 collected, and then 1cm of each tissue was opened longitudinally and washed briefly in PBS before
779 homogenization. For the purposes of this study, the small intestinal and large intestinal gut-
780 associated lymphoid tissue (S.I. and L.I. GALT) was collected by removing the lining of the tissues
781 (including the fat) for each of the small intestine and large intestine. For analysis of bacterial loads in
782 the blood, 100 µl of blood was aspirated from the heart immediately after euthanasia and collected
783 in PBS with 2% BSA and 1 mM EDTA. Blood samples were also homogenized. Dissection tools were
784 disinfected in 70% EtOH in between each organ to minimize the chance of cross-contamination
785 between organs.
786
787 **Analysis of population dynamics using neutral sequence tags**

Mice were infected with an equal ratio of *S.*Tm 14028S Sm^R recipient strains (total ~10^3 CFU) bearing sequence tags at a neutral locus in the chromosome (Grant et al., 2008). For analysis of re-seeding and plasmid transfer dynamics in **Fig. 2**, three recipient tagged strain were used (TAG1-3 Kan^R; 1:1:1 ratio). On day 2 post infection, an equal ratio of donor tagged strains (*S.*Tm $SL1344^{Avir}$ $P2^{TAG}$ strains; TAG4-7 Cm^R; 1:1:1:1) were given at a total inoculum size of ~$5x10^7$ CFU per mouse orally. The inocula were enriched in either LB+chloramphenicol (for donors) or LB+kanamycin (for recipients). At the end of the experiment (i.e., on day 10 post infection), mice were euthanized and recipient+transconjugant populations were enriched from 100 µl of the feces and organ homogenates (in parallel to selective plating) in LB supplemented with kanamycin.

For analysis of re-seeding dynamics in the presence or absence of donors (**Fig. 1-figure supplement 4; Fig. 2-figure supplement 2**), an equal ratio of *S.*Tm 14028S Sm^R recipient strains (total ~10^3 CFU) bearing 7 sequence unique tags at a neutral locus in the chromosome were used.

Enrichments were concentrated and genomic DNA was extracted using a QIAamp DNA Mini Kit (Qiagen). qPCR analysis was performed according to temperature conditions as previously described (Grant et al., 2008) using qPCR primers specific to the TAG and a universal second primer, *ydgA* (**Table 3**). The relative proportion was calculated by dividing the DNA copy number (calculated from the C_T value) of each tag detected, by the sum of all 7 tags in the sample. A dilution standard of purified chromosomal DNA allowed for a correlation between DNA copy number and C_T value. For each qPCR run, the detection limit was determined by the C_T value of the most-diluted DNA standard. The least precise detection limit defines the conservative detection limit plotted on graphs and used for the mathematical model ($8.9x10^{-5}$). Once the relative proportion was determined, recipient tags were separated from plasmid tags (however, the proportion remains relative to all tags). This data is presented in **Fig. 2-figure supplement 1**. Next, the tags were sorted according to the most abundant in the feces in each given mouse (separately for recipient and plasmid tags). This ranking was conserved for analysis in other organs to allow a correlation between the most abundant tag in the organs relative to the feces. For example, if TAG2 appeared the most abundant in the feces but least abundant in the mLN, it would ranked and coloured according to the most abundant tag, and it would still appear the same colour in the mLN, despite it not being the most abundant tag in the mLN. This data is presented in **Fig. 2A-B**. The samples in **Fig. 2-figure supplement 2** were analyzed the same, but were not sorted according to the most abundant tag in the feces, and is instead presented as raw tag proportions relative to all 7 recipient chromosomal tags.

Measurement of fecal ampicillin

Detection and absolute quantification of ampicillin was carried out using high-performance liquid chromatography heated electrospray ionization high-resolution mass spectrometry (HPLC HESI HRMS). Fecal samples were homogenized in PBS and immediately frozen after collection. Prior to analysis, samples were thawed and centrifuged at high speed. The supernatants were analyzed on a Dionex UltiMate 3000 HPLC coupled to a Q Exactive™ Hybrid Quadrupole-Orbitrap™ mass spectrometer. Chromatographic separation was obtained on a Phenomenex Kinetex 2.6 µm XB-C18 150 × 4.6 mm column at 30°C. Water (A) and acetonitrile (B), each containing 0.1% formic acid, were employed as mobile phases. A gradient of total 12.5 min was applied at a flowrate of 800 µL/min, starting with 3% B for 2 min, 3% to 50% B in 3 min, 50% to 98% B in 5 min, 98% B for 1 min, 98% to 3% B in 1 min and 3% B for 0.5 min. MS-settings: spray voltage (+) 3.5 kV, capillary temperature 320 °C; sheath gas (57.50), auxiliary gas (16.25), sweep gas (3.25); probe heater 462.50°C; S-Lens RF (50), resolution (70.000); AGC target (3e6), microscans (1), maximum IT 200 ms, scan range 250–750 *m/z.* For quantification, an ampicillin standard curve was recorded using H_2O diluted concentrations of 10 ng/mL, 100 ng/mL, 500 ng/mL, 1 µg/mL, 10 µg/mL and 100 µg/mL from a 1 mg/mL ampicillin stock

solution. Samples were analyzed by retention time of ampicillin and the respective ion adduct $[M+H]^+$ = 350.1169 *m/z* with a mass tolerance of 5 ppm. 15 µL of each sample were injected and ampicillin concentrations were calculated using the Thermo Xcalibur 2.2 Quan Browser software. The concentration given in µg/ml of supernatant was normalized to the weight of feces collected and converted to µg/ml fecal content using the average density of feces (Brown et al., 1996).

Statistical analysis

Statistical tests on experimental data were performed using GraphPad Prism 8 for Windows. The specific test used is each figure is described in the figure caption (a test is only indicated if statistics were used). The mathematical model was fit to the experimental measurements using an Approximate Bayesian Computation (ABC) approach (Marjoram et al., 2003). For the fit, we considered three sets of summary statistics: the skew of the plasmid and chromosomal tag distributions, the total size of the transconjugant and recipient population on day 10, and the time at which the transconjugant and recipient populations first exceeded 10^6 CFU/g feces. A simulation was called "successful" if all summary statistics were within three standard deviations of the experimentally observed mean of these statistics. Migration and conjugation rates were varied on a grid, all other parameters were kept fixed (**Supplementary table S1**). All R-code needed to simulate the stochastic model, estimate the most likely parameters from the experimental data, and plot the results, is included in the Github repository https://github.com/JSHuisman/Recorder .

Acknowledgements:

We would like to thank the staff at RCHCI and EPIC animal facilities, and members of the Hardt, Sunagawa and Slack labs for helpful discussions. We would also like to acknowledge the reviewers for their constructive feedback and helpful suggestions to improve this manuscript.

Funding:

This work has been supported by grants from the Swiss National Science Foundation (NRP 72 407240_167121, 310030B_173338 and 310030_192567), the Gebert Rüf Foundation (GRS-060/18) and the Monique Dornonville de la Cour Foundation to WDH. MD is funded by an SNF professorship grant (PP00PP_176954) and a BRCCH multi-investigator grant, JSH is funded by NRP72 grant 407240-167121 from the Swiss National Science Foundation, and EB acknowledges a Boehringer Ingelheim Fonds PhD fellowship.

Contributions:

EB and WDH conceived the project and designed the experiments. EB, JAH, YS, EG, and JPMN carried out the mouse experiments and analyzed data. JSH designed and performed the mathematical modeling. RRR and SB supervised the mathematical modelling. AOB and JP measured fecal ampicillin using mass spectrometry. EB wrote the initial draft of the manuscript. EB, MD, and WDH reviewed and edited the manuscript to its final form. All authors read, commented on, and approved this manuscript.

Competing interests statement:

The authors declare no conflicts of interest.

Supplementary information:

Description of the mathematical model

We model the re-seeding of Salmonella recipients from systemic sites into the gut, and the subsequent creation of transconjugants through plasmid transfer from donors. We follow the dynamics of Donor (D), Recipient (R), and Transconjugant (T) populations in the gut. These populations are further divided into isogenic subpopulations based on their sequence tags. The donors D_j carry a plasmid tag $j \in 1 \ldots N_j$, where N_j is the number of plasmid tags ($N_j = 4$). Recipients R_i carry a chromosomal tag $i \in 1 \ldots N_i$, where N_i is the total number of chromosomal tags ($N_i = 3$). Transconjugants T_{ij} carry both a chromosomal and a plasmid tag.

To describe the dynamics of these populations, we make several assumptions. Recipients are introduced into the gut at an overall rate μ. Here we assume this rate is constant, although it likely increases slightly during the experiment as a function of the recipient population size at systemic sites. We assume the populations of recipients and donors in the gut are well-mixed, and plasmid transfer is described by mass-action kinetics. Plasmids are thus transferred between donors and recipients at a constant per-contact rate γ_D. Once transconjugants are formed, these can also transfer their plasmid at a constant per-contact rate γ_T. All plasmids are isogenic; they transfer from donors or transconjugants at the same rate and can be transferred only to naïve recipients.

Resources are limited in the gut, so we model bacterial population growth as a logistic function of the population size. We assume the donor population is limited by a different resource than the recipient and transconjugant populations, since they are not isogenic (Lee et al., 2013). The populations thus reach separate carrying capacities, denoted by K_D and K_{RT} respectively. Otherwise, the growth dynamics are assumed population independent: the bacteria are born at a birth-rate r, are cleared at a clearance rate c (this includes both death and efflux from the gut), and similar to (Bakkeren et al., 2019) we parametrize this with a residual birth-rate at carrying capacity $r_K = c$ (to ensure some continued population turnover even at high densities).

We simulate the population dynamics stochastically using the tau-leaping method from the R package *adaptivetau* (Johnson, 2016). The corresponding deterministic equations (in the limit of large numbers) are:

$$\dot{D_j} = (r + r_K)D_j - D_j\left(c + \mathrm{r}\frac{\sum_j D_j}{K_D}\right) \#(1)$$

$$\dot{R_i} = (r + r_K)R_i + \frac{1}{N_i}\mu - \sum_j\left(\gamma_D D_j + \gamma_T \sum_i T_{ij}\right)R_i - R_i\left(c + \mathrm{r}\frac{\sum_i(R_i + \sum_j T_{ij})}{K_{RT}}\right) \#(2)$$

$$\dot{T_{ij}} = (r + r_K)T_{ij} + \left(\gamma_D D_j + \gamma_T \sum_i T_{ij}\right)R_i - T_{ij}\left(c + \mathrm{r}\frac{\sum_i(R_i + \sum_j T_{ij})}{K_{RT}}\right) \#(3)$$

Parametrizing the mathematical model

In the main simulations, we varied the migration rate μ and the conjugation rates $\gamma_{D/T}$ while the other parameters were kept fixed (summarized in **Table S1**). The population-independent parameters describing the bacterial growth dynamics (*r, c,* r_K*),* as well as the carrying capacities $K_{D/RT}$ and inoculum density D_0, were set to the values from (Bakkeren et al., 2019) . There they were parametrized based on experimental data from the same mouse model system (Barthel et al., 2003; Moor et al., 2017). The number of distinguishable chromosomal and plasmid tag populations match

those used in this paper. We fixed the conjugation rates from donors and transconjugants to the same value, and the carrying capacities of donors and recipients+transconjugants were set to the same value.

Table S1. Parameter values used in the simulations

Parameter	Function	Value	Units
r	Birth-rate	44 ln(2)	Per day
c	Clearance-rate	4 ln(2)	Per day
r_K	Residual birth-rate at carrying capacity	$4\ln(2)$	Per day
$K = K_{D/RT}$	Carrying capacity	10^9	CFU/g feces
D_0	Size of the donor inoculum	10^7	CFU/g feces
N_i	Number of distinguishable chromosomal tags	3	Dimensionless
N_j	Number of distinguishable plasmid tags	4	Dimensionless
μ	Re-seeding rate of recipients from systemic sites	**Uniform on the discrete grid** 10^{-6} – 10^3 in 0.25 log increments	CFU/g feces per day
$\gamma = \gamma_{D/T}$	The rate of conjugation from donors or transconjugants per mating pair	**Uniform on the discrete grid** 10^{-12} – 10^{-3} in 0.25 log increments	Per CFU/g feces per day

Parameter estimation in the mathematical model

We use Approximate Bayesian Computation (ABC) (Marjoram et al., 2003) to infer the most likely values of migration rate μ and conjugation rate γ. We varied both parameters on a grid, running 100 simulations per parameter set. For each parameter combination, we calculated summary statistics (see below) to compare the simulations to the experimental data.

i. The Evenness index E of the plasmid and chromosomal tag distributions. E is defined as 1 – g where g is the Gini index (Bakkeren et al., 2019; Maier et al., 2014).
ii. The size of the recipient and transconjugant populations on day 10, respectively.
iii. The time at which the recipient and transconjugant populations first exceed 10^6 CFU/g feces, respectively.

For **Fig. 2C** we calculated the likelihood of the parameter combination as the percentage of simulations that return all summary statistics within three standard deviations of the experimentally observed mean of these statistics. The experimental data used to calculate the mean of these statistics is derived from **Fig. 1B, Fig. 1-figure supplement 1,** and **Fig. 2A-B** (n=8)**.** Due to the assumptions of our model, we excluded mice where re-seeding did not occur. Therefore, the migration rate calculated here may be slightly overestimated. However, we do not expect the relative importance of re-seeding or conjugation to change due to the exclusion of these mice.

Table S2. Parameter estimates

Simulation	Maximum likelihood (μ,γ) pair	μ value from the marginal posterior distribution	γ value from the marginal posterior distribution

Main text (**Fig. 2C**)	μ=1.78 (CFU/g feces per day) γ=3.16×10^{-11} (per CFU/g feces per day)	7.1 (CFU/g feces per day) HPD: [0.03, 31.6]	9.36×10^{-10} (per CFU/g feces per day) HPD: [1×10^{-12}, 5.6×10^{-9}]

*HPD: Highest posterior density interval

Translation into per-recipient rates

In the mathematical model, the dynamic parameters describing migration and conjugation (μ, $\gamma_{D/T}$) are reported in different units. To facilitate their direct comparison we can approximate the relative magnitude of these rates per recipient per day.

Recipient migration was inferred to result in 1.78 recipient CFU/g feces per day. This should be divided by the total population of recipients in systemic reservoirs (8.5 x 10^5 ; Fig. 1C) to obtain a per-recipient probability of migration. These values result in an approximate probability per recipient (tissue-located) of 2.1 x 10^{-6} per day.

In contrast, γ is a rate constant that needs to be multiplied by two population sizes to be comparable with the migration rate, μ. To obtain a per-recipient (gut-located) conjugation rate reported as CFU/g feces per day, γ needs to be multiplied by the size of the donor population in the gut. Assuming a donor population of 10^9, this results in conjugation rates of 3.2 x 10^{-2} per day.

Dependence of transconjugant emergence on the carrying capacity in the gut

In a separate analysis, we estimated the evenness of the plasmid and chromosomal tag distributions, as well as the final recipient and transconjugant population sizes, as a function of the carrying capacity. Here we fixed the migration rate μ and conjugation rate γ at their most likely values (μ = 1.78 CFU/g feces per day, γ = 3.16×10^{-11} per CFU/g feces per day), and varied the carrying capacity K uniformly on the grid $10^3 - 10^{10}$ in 0.25 log increments.

In addition, we repeated this set of simulations with a conjugation rate that was either 100-fold higher, or 100-fold lower than the most likely value, to illustrate a range of plausible plasmid conjugation rates (Benz et al., 2020).

970 **Supplementary figure captions**
971
972 **Fig. 1-figure supplement 1. Fecal populations for mice in Figure 1.** Donors (blue; Cm^R), recipients
973 (green; Kan^R), and transconjugants (red; Cm^R and Kan^R) were enumerated by selective and/or replica
974 plating on MacConkey agar. The black dotted lines represent the detection limits for transconjugants
975 and donors (and recipients in **panel B**). The green dotted lines represent the detection limits for
976 recipients. The detection limit is higher for recipients once the density of bacteria reaches $>10^8$ CFU/g
977 feces (because of the limit of colonies on a plate for replica plating). Before this happens, recipient
978 populations can appear below this line (then the black dotted line is the detection limit). Lines of
979 colour connect medians between days. **A-B)** Mice from **Fig. 1B-C** infected with $SL1344^{Avir}$ $P2^{cat}$ as
980 donors. **A)** Mice infected with *S.*Tm^{WT} recipients (n=13). **B)** Mice infected with *S.*Tm^{SPI-2} recipients
981 (n=8). **C)** Mice from **Fig. 1D-E** infected with *S.*Tm^{WT} recipients and *E. coli* 536 $P2^{cat}$ as donors (n=12).
982
983 **Fig. 1-figure supplement 2. Verification of transconjugant formation by colony PCR.** 4 donor clones,
984 4 recipient clones, and 10 transconjugant clones were isolated from mice on day 10 of the
985 experiment in **Fig. 1-figure supplement 4** (either feces or the mesenteric lymph node; mLN; the
986 individual mice are labelled the same as in **Fig. 2-figure supplement 2**) according to the resistance
987 profile used to classify subpopulations (donors = Cm^R; recipients = Kan^R; transconjugants =
988 Cm^R+Kan^R). A colony PCR was performed using primers specific to either the 14028S recipient
989 chromosome (top) or the $P2^{cat}$ conjugative plasmid (bottom), and PCR products were run on a 1%
990 agarose gel.
991
992 **Fig. 1-figure supplement 3. TTSS-1-dependent invasion of recipients is not necessary for re-seeding.**
993 **A)** Mice were i.p. infected with 10^3 CFU of 14028S Sm^R *invG* (TTSS-1-deficient encoded on SPI-1;
994 *S.*Tm^{SPI-1}; n=5). On day 2 post infection, 25 mg of streptomycin was given. Selective plating was used
995 to determine the fecal loads for 10 days. **B)** Tissue reservoirs of *S.*Tm at day 10 of the experiment.
996 Organs of mice in **panel A** were analyzed for *S.*Tm population sizes using selective plating on
997 MacConkey agar. GB = gall bladder; mLN = mesenteric lymph node. **A-B)** Bars or solid lines indicate
998 median. Dotted lines indicate the detection limit.
999
1000 **Fig. 1-figure supplement 4. Donor inoculation does not promote re-seeding.** Mice were i.p. infected
1001 with 10^3 CFU of a 1:1:1:1:1:1:1 mix of 14028S Sm^R *TAG1-7*. On day 2 post infection, 20 mg of
1002 streptomycin was given. 4 hours later $5x10^7$ CFU of *S.*Tm^{Avir} (*invG ssaV* mutant) $P2^{cat}$ were given to
1003 half the mice (with donors; solid black circles; n=4) and half the mice were left untreated (without
1004 donors; hollow black circles; n=5). **A)** Selective plating was used to determine the re-seeding
1005 population (Kan^R colonies, which includes the transconjugant population in same cases). Bars
1006 indicate the median. **B)** Tissue reservoirs of *S.*Tm recipients at day 10. Organs of mice in **panel A** were
1007 analyzed for the total 14028S population (recipients + transconjugants; Kan^R). Lines indicate median.
1008 GB = gall bladder; mLN = mesenteric lymph node. **A-B)** Dotted line indicates the detection limit. A
1009 two-tailed Mann Whitney-U test was used to compare mice with donors (solid circles) to mice
1010 without donors (hollow circles) in each sample ($p>0.05$ not significant (ns)). **C)** Fecal population of
1011 donors (blue), recipients (green), and transconjugants (red) for the mice in **panel A and B** with
1012 donors. Selective and/or replica plating was used to determine these subpopulations. The black
1013 dotted lines represent the detection limits for transconjugants and donors. The green dotted lines
1014 represent the detection limits for recipients. The detection limit is higher for recipients once the
1015 density of bacteria reaches $>10^8$ CFU/g feces (because of the limit of colonies on a plate for replica
1016 plating). Before this happens, recipient populations can appear below this line (then the black dotted
1017 line is the detection limit). Lines of colour connect medians between days.
1018

1019 **Fig. 1-figure supplement 5. Control for re-seeding and obtaining a plasmid from persisters induced**
1020 **by antibiotic treatment.** Mice were i.p. infected with 10^3 CFU of 14028S Sm^R *TAG1* (Kan^R; n=7). On
1021 day 2 post infection, doses of ceftriaxone (1.5 mg i.p. per mouse per day) were given for three
1022 consecutive days. On day 6, 20 mg of streptomycin was given 4 hours before $5x10^7$ CFU of *E. coli* 536
1023 $P2^{cat}$ (Cm^R). *E. coli* was given again on day 8 post infection to ensure colonization. **A)** Donors (blue;
1024 Cm^R), recipients (green; Kan^R), and transconjugants (red; Cm^R and Kan^R) were enumerated by
1025 selective and/or replica plating on MacConkey agar. The black dotted lines represent the detection
1026 limits for transconjugants and donors. The green dotted lines represent the detection limits for
1027 recipients. The detection limit is higher for recipients once the density of bacteria reaches $>10^8$ CFU/g
1028 feces (because of the limit of colonies on a plate for replica plating). Before this happens, recipient
1029 populations can appear below this line (then the black dotted line is the detection limit). Lines of
1030 colour connect medians between days. **B)** Organs of mice in **panel A** were analyzed for population
1031 sizes of recipients and transconjugants. Lines indicate medians. Dotted line indicates the detection
1032 limit. GB = gall bladder; mLN = mesenteric lymph node.
1033
1034 **Fig. 1-figure supplement 6. Localization of tissue reservoirs of *S.*Tm prior to re-seeding.** Mice (n=7)
1035 were i.p. infected with 10^3 CFU of a 1:1:1:1:1:1:1 mix of 14028S Sm^R *TAG1-7*. At day 2 post infection,
1036 *S.*Tm in the organs were enumerated. For feces and the intestinal content, pre-weighed tubes were
1037 used to determine *S.*Tm per g of content. Blood is reported per ml. Intestinal tissues are reported per
1038 cm. The small intestinal (S.I.) and large intestinal (L.I.) gut-associated lymphoid tissues (GALT) contain
1039 the lining of the intestinal tissues, which includes the GALT (but also fat). Here, we called them S.I.
1040 and L.I. GALT, but they can contain more than just this region. Dotted lines indicate the detection
1041 limits. Lines indicate medians.
1042
1043 **Fig. 2-figure supplement 1**. **Raw tag proportions before sorting and re-colouring for mice in Figure**
1044 **2.** Relative tag proportions detected by qPCR in the inocula (R. ino. = recipient inoculum; D. ino. =
1045 donor inoculum), the feces, and the organs at day 10 of the experiment. All samples are derived
1046 from an enrichment in LB+kanamycin (to enrich for recipients+transconjugants). Each tag is given a
1047 unique colour. Mice are separated by vertical dashed lines. Sample groups are separated by vertical
1048 solid lines. Dotted line indicates the conservative detection limit. GB = gall bladder; mLN =
1049 mesenteric lymph node. **A)** Recipient tags. **B)** Plasmid tags.
1050
1051 **Fig. 2-figure supplement 2**. **Distribution of tag proportions dependent on the presence or absence**
1052 **of donors. Further analysis of mice in Fig. 1-figure supplement 4.** Relative tag proportions detected
1053 by qPCR in the inocula (R. ino. = recipient inoculum), the feces, and the organs at day 10 of the
1054 experiment. All samples are derived from an enrichment in LB+kanamycin (to enrich for
1055 recipients+transconjugants). Each tag is given a unique colour. Mice are separated by vertical dashed
1056 lines. Sample groups are separated by vertical solid lines. Dotted line indicates the conservative
1057 detection limit. If a tag was not detected or below 10^{-8}, it was set to a proportion of 10^{-8} for better
1058 visualization of tag skew. Grey fill indicates samples where no enrichments could be taken because
1059 there were no Kan^R *S.*Tm. GB = gall bladder; mLN = mesenteric lymph node. **A)** Mice without donors.
1060 **B)** Mice with donors.
1061
1062 **Fig. 2-figure supplement 3. Summary statistics used for fitting the mathematical model to the**
1063 **experimental data in Fig. 2C. A-F)** The mathematical model was fit to the experimental data using 6
1064 metrics (described in the **Supplementary information**). The values of all 6 metrics were calculated on
1065 the grid of possible migration and conjugation rate pairs. For each metric, the experimentally
1066 determined mean is shown in red (an arrow and red text indicates the mean value), and values of
1067 simulations that are above the experimental mean are indicated in a gradient towards white,

1068 whereas values that are below the experimental mean are indicated in a gradient towards black.
1069 Grey fill indicates migration and conjugation rate pairs where the given metric cannot be calculated
1070 (e.g. evenness of tags cannot be calculated if re-seeding of recipients into the feces does not occur;
1071 the recipient population never reaches appreciable densities if the conjugation rate is too high). **A)**
1072 Evenness of chromosomal tags in the recipient+transconjugant fecal population at day 10
1073 (experimental mean = 0.0166; SD = 0.0508). **B)** Evenness of plasmid tags in the transconjugant fecal
1074 population at day 10 (experimental mean = 0.358; SD = 0.282). **C)** Days of the experiment (timeline as
1075 in **Fig. 1**) until the recipient population exceeds 10^6 CFU / g feces (experimental mean = 4.875; SD =
1076 1.642). **D)** Days of the experiment (timeline as in **Fig. 1**) until the transconjugant population exceeds
1077 10^6 CFU/g feces (experimental mean = 5.00; SD = 0.926). **E)** Recipient population in the feces at day
1078 10 (experimental mean = $2.9x10^8$ CFU/g feces; SD = $3.75x10^8$ CFU/g feces). **F)** Transconjugant
1079 population in the feces at day 10 (experimental mean = $2.61x10^8$ CFU/g feces; SD = $3.45x10^8$ CFU/g
1080 feces).
1081
1082 **Fig. 2-figure supplement 4. Dependence of recipient and transconjugant population sizes on the**
1083 **carrying capacity with a higher or lower conjugation rate compared to Fig. 2D, and correlation with**
1084 **experimental data in Fig. 1. A-B)** Transconjugant invasion increases proportional to the carrying
1085 capacity, as a proxy for colonization resistance provided by the microbiota. Correlation of the donor
1086 population size at day 10 (as a measure for carrying capacity; either SL1344 *S.*Tm^{Avir} or *E. coli* 536;
1087 data from **Fig. 1-figure supplement 1A, C;** n=25) to the transconjugant population in the feces **(panel**
1088 **A;** data from **Fig. 1-figure supplement 1A, C**) or mesenteric lymph node (mLN; **panel B**; data from **Fig.**
1089 **1C, E**). Dotted lines indicate the detection limits by selective plating. A line of best fit is shown and a
1090 linear regression is performed: **A)** R^2 = 0.5604; F test determined non-zero slope (p<0.0001); **B)** R^2 =
1091 0.4913; F test determined non-zero slope (p<0.0001). **C-D**) Simulation data. The migration rate was
1092 fixed to the most likely values in **Fig. 2C**, but the conjugation rate was fixed to $3.16x10^{-9}$, 100-fold
1093 higher than in **Fig. 2D** to test the case of a plasmid with a higher conjugation rate **(panel C),** or fixed
1094 to $3.16x10^{-13}$, 100-fold lower than in **Fig. 2D** to test the case of a plasmid with a lower conjugation
1095 rate **(panel D)**. The carrying capacity was varied. Recipient (green) and transconjugant (red)
1096 populations at the end of the simulation (day 10; n=100 simulations per carrying capacity) are shown
1097 as the mean with the range of values. The lowest value was set to 1 CFU/g feces to allow visualization
1098 on a log scale. The grey dotted lines correspond to the carrying capacity at which transconjugants are
1099 present at 10^6 CFU/g feces, as a density threshold that we speculate should facilitate some frequency
1100 of invasion into tissue reservoirs.
1101
1102 **Fig. 3-figure supplement 1. Additional fecal and organ populations for mice in Figure 3. A-B)**
1103 Secondary conjugation experiment (circles); mice in **Fig. 3A-B**. Donors (blue; Cm^R), primary recipients
1104 (green; Kan^R), primary transconjugants (red; Cm^R and Kan^R), secondary recipients (beige; Amp^R), and
1105 secondary transconjugants (black; Amp^R and Cm^R) were enumerated by selective and/or replica
1106 plating on MacConkey agar. **B)** Organs of mice in **panel A** were analyzed for population sizes of
1107 donors, recipients and transconjugants. **C-D)** Multiple plasmids experiment (squares); mice in **Fig. 3C-**
1108 **D**. $P2^{cat}$ donors (blue; Cm^R), recipients (green; Kan^R), $P2^{cat}$ transconjugants (red; Cm^R and Kan^R), pESBL
1109 donors (purple; Amp^R), and pESBL transconjugants (grey; Amp^R and Kan^R) were enumerated by
1110 selective and/or replica plating on MacConkey agar. **D)** Organs of mice in **panel A** were analyzed for
1111 population sizes of donors, recipients and transconjugants. **A,C)** The black dotted lines represent the
1112 detection limits for transconjugants and donors. The green dotted lines represent the detection
1113 limits for recipients. The detection limit is higher for recipients once the density of bacteria reaches
1114 $>10^8$ CFU/g feces (because of the limit of colonies on a plate for replica plating). Before this happens,
1115 recipient populations can appear below this line (then the black dotted line is the detection limit).

1116 Lines of colour connect medians between days. **B,D)** Lines indicate medians. Dotted line indicates the
1117 detection limit. GB = gall bladder; mLN = mesenteric lymph node.
1118
1119 **Fig. 3-figure supplement 2. Control that *E. coli* donors are not detected in tissue reservoirs after**
1120 **antibiotic treatment.** Mice (n=5) were i.p. infected with 10^3 CFU of 14028S Sm^R *TAG1* recipients
1121 (Kan^R) and $5x10^7$ CFU of *E. coli* 536 $P2^{cat}$ donors (Cm^R) as in **Fig. 3**. Selective plating and colony colour
1122 on MacConkey agar was used to determine population sizes of donors (blue), recipients (green), and
1123 transconjugants (red; Cm^R and Kan^R). On day 10, mice were given 3 mg ciprofloxacin for three days in
1124 a row, along with 2 g/l ampicillin in the drinking water from day 11-15. **A)** Fecal population sizes. The
1125 black dotted lines represent the detection limits for transconjugants and donors. The green dotted
1126 lines represent the detection limits for recipients. The detection limit is higher for recipients once the
1127 density of bacteria reaches $>10^8$ CFU/g feces (because of the limit of colonies on a plate for replica
1128 plating). Before this happens, recipient populations can appear below this line (then the black dotted
1129 line is the detection limit). Lines of colour connect medians between days. **B)** Organs of mice in **panel**
1130 **A** were analyzed for population sizes of donors, recipients and transconjugants. Lines indicate
1131 medians. Dotted line indicates the detection limit. GB = gall bladder; mLN = mesenteric lymph node.
1132
1133 **Fig. 3-figure supplement 3. Further control experiment to determine that *E. coli 536* cannot form**
1134 **persister reservoirs in host tissues.** Mice (n=5) were streptomycin treated (20 mg oral dose) 4 hours
1135 before oral gavage of $5x10^7$ CFU of *E. coli* 536 $P2^{cat}$ donors (Cm^R). On day 8, mice were given 3 mg
1136 ciprofloxacin for three days in a row, along with 2 g/L ampicillin in the drinking water from day 9-13.
1137 This protocol follows the same treatment regime as in **Fig. 3** relative to the colonization time of the *E.*
1138 *coli* 536 donors. Mice were switched to streptomycin drinking water (1 g/L) from day 13-16 to select
1139 for any remaining *E. coli* 536 until the end of the experiment. **A)** Selective plating was used to
1140 determine fecal population sizes of *E. coli* 536. Lines connect medians. **B)** Tissue reservoirs were
1141 analyzed by selective plating on day 16 of the experiment. GB = gall bladder; mLN = mesenteric
1142 lymph node. Lines indicate the median. **A-B**) Dotted lines indicate the detection limit.
1143
1144 **Fig. 3-figure supplement 4. Conjugation is not detectable within host tissue reservoirs.** Mice (n=5)
1145 were i.p. infected with both SL1344 $P2^{cat}$ donors (blue) and 14028S Sm^R recipients (Kan^R; green)
1146 sequentially (5 minutes apart; ~10^3 CFU total). On day 3, mice were euthanized, and tissue reservoirs
1147 were analyzed for transconjugant formation (red). Dotted lines indicate the detection limit by
1148 selective plating. Lines indicate media.
1149
1150 **Fig. 4-figure supplement 1. *E. coli* population sizes and total *S.*Tm population sizes in tissue**
1151 **reservoirs of mice in Fig. 4. A)** *E. coli* $P2^{cat}$ (Cm^R) and *E. coli* pESBL (Amp^R) populations were
1152 enumerated by selective plating and colour on MacConkey agar. Coloured lined connect medians. **B)**
1153 Total *S.*Tm populations (Kan^R) in organs were determined by selective plating on kanamycin
1154 MacConkey agar. GB = gall bladder; mLN = mesenteric lymph node. Lines indicate the media. **A-B)** A
1155 two-tailed Mann Whitney-U test was used to compare $S.Tm^{WT}$ + *E. coli* $P2^{cat}$ (black; n=10) to $S.Tm^{WT}$ +
1156 *E. coli* $P2^{cat}$ (orange; n=10) in each sample ($p>0.05$ not significant (ns), $p<0.05$ (*), $p<0.01$ (**),
1157 $p<0.0001$ (****)). Dotted lines indicate the detection limits.
1158
1159

1160 **References:**

1161

1162 Ackermann, M., Stecher, B., Freed, N. E., Songhet, P., Hardt, W. D., & Doebeli, M. (2008). Self-
1163 destructive cooperation mediated by phenotypic noise. *Nature*, *454*(7207), 987-990.
1164 https://doi.org/nature07067 [pii]

1165 10.1038/nature07067
1166 Bajaj, P., Singh, N. S., & Virdi, J. S. (2016). Escherichia coli beta-Lactamases: What Really Matters.
1167 *Front Microbiol*, *7*, 417. https://doi.org/10.3389/fmicb.2016.00417
1168 Bakkeren, E., Diard, M., & Hardt, W. D. (2020). Evolutionary causes and consequences of bacterial
1169 antibiotic persistence. *Nat Rev Microbiol*. https://doi.org/10.1038/s41579-020-0378-z
1170 Bakkeren, E., Gül, E., Huisman, J. S., Steiger, Y., Rocker, A., Hardt, W.-D., & Diard, M. (2021).
1171 Cooperative virulence can emerge via horizontal gene transfer but is stabilized by
1172 transmission. *bioRxiv*, 2021.2002.2011.430745. https://doi.org/10.1101/2021.02.11.430745
1173 Bakkeren, E., Huisman, J. S., Fattinger, S. A., Hausmann, A., Furter, M., Egli, A., Slack, E., Sellin, M. E.,
1174 Bonhoeffer, S., Regoes, R. R., Diard, M., & Hardt, W. D. (2019). Salmonella persisters promote
1175 the spread of antibiotic resistance plasmids in the gut. *Nature*, *573*(7773), 276-280.
1176 https://doi.org/10.1038/s41586-019-1521-8
1177 Balaban, N. Q., Helaine, S., Lewis, K., Ackermann, M., Aldridge, B., Andersson, D. I., Brynildsen, M. P.,
1178 Bumann, D., Camilli, A., Collins, J. J., Dehio, C., Fortune, S., Ghigo, J. M., Hardt, W. D., Harms,
1179 A., Heinemann, M., Hung, D. T., Jenal, U., Levin, B. R., Michiels, J., Storz, G., Tan, M. W.,
1180 Tenson, T., Van Melderen, L., & Zinkernagel, A. (2019). Definitions and guidelines for
1181 research on antibiotic persistence. *Nat Rev Microbiol*. https://doi.org/10.1038/s41579-019-
1182 0196-3
1183 Barthel, M., Hapfelmeier, S., Quintanilla-Martinez, L., Kremer, M., Rohde, M., Hogardt, M., Pfeffer, K.,
1184 Russmann, H., & Hardt, W. D. (2003). Pretreatment of mice with streptomycin provides a
1185 *Salmonella* enterica serovar Typhimurium colitis model that allows analysis of both pathogen
1186 and host. *Infect Immun*, *71*(5), 2839-2858. http://www.ncbi.nlm.nih.gov/pubmed/12704158
1187 Benz, F., Huisman, J. S., Bakkeren, E., Herter, J. A., Stadler, T., Ackermann, M., Diard, M., Egli, A., Hall,
1188 A. R., Hardt, W. D., & Bonhoeffer, S. (2020). Plasmid- and strain-specific factors drive
1189 variation in ESBL-plasmid spread in vitro and in vivo. *ISME J*. https://doi.org/10.1038/s41396-
1190 020-00819-4
1191 Berger, H., Hacker, J., Juarez, A., Hughes, C., & Goebel, W. (1982). Cloning of the chromosomal
1192 determinants encoding hemolysin production and mannose-resistant hemagglutination in
1193 Escherichia coli. *J Bacteriol*, *152*(3), 1241-1247.
1194 https://www.ncbi.nlm.nih.gov/pubmed/6754701
1195 Brown, D. M., Butler, D., Orman, N. R., & Davies, J. W. (1996). Gross solids transport in small
1196 diameter sewers. *Water Science and Technology*, *33*(9), 25-30.
1197 https://doi.org/https://doi.org/10.1016/0273-1223(96)00366-6
1198 Brzuszkiewicz, E., Bruggemann, H., Liesegang, H., Emmerth, M., Olschlager, T., Nagy, G., Albermann,
1199 K., Wagner, C., Buchrieser, C., Emody, L., Gottschalk, G., Hacker, J., & Dobrindt, U. (2006).
1200 How to become a uropathogen: comparative genomic analysis of extraintestinal pathogenic
1201 Escherichia coli strains. *Proc Natl Acad Sci U S A*, *103*(34), 12879-12884.
1202 https://doi.org/10.1073/pnas.0603038103
1203 Carattoli, A. (2009). Resistance plasmid families in Enterobacteriaceae. *Antimicrob Agents*
1204 *Chemother*, *53*(6), 2227-2238. https://doi.org/10.1128/AAC.01707-08
1205 Claudi, B., Sprote, P., Chirkova, A., Personnic, N., Zankl, J., Schurmann, N., Schmidt, A., & Bumann, D.
1206 (2014). Phenotypic variation of Salmonella in host tissues delays eradication by antimicrobial
1207 chemotherapy. *Cell*, *158*(4), 722-733. https://doi.org/10.1016/j.cell.2014.06.045
1208 Cully, M. (2014). Public health: The politics of antibiotics. *Nature*, *509*(7498), S16-17.
1209 https://doi.org/10.1038/509S16a

1210 Cunrath, O., & Bumann, D. (2019). Host resistance factor SLC11A1 restricts Salmonella growth
1211 through magnesium deprivation. *Science*, *366*(6468), 995-999.
1212 https://doi.org/10.1126/science.aax7898
1213 D'Costa, V. M., McGrann, K. M., Hughes, D. W., & Wright, G. D. (2006). Sampling the antibiotic
1214 resistome. *Science*, *311*(5759), 374-377. https://doi.org/10.1126/science.1120800
1215 Datsenko, K. A., & Wanner, B. L. (2000). One-step inactivation of chromosomal genes in Escherichia
1216 coli K-12 using PCR products. *Proc Natl Acad Sci U S A*, *97*(12), 6640-6645.
1217 https://doi.org/10.1073/pnas.120163297
1218 Davies, J., & Davies, D. (2010). Origins and evolution of antibiotic resistance. *Microbiol Mol Biol Rev*,
1219 *74*(3), 417-433. https://doi.org/10.1128/MMBR.00016-10
1220 Desai, P. T., Porwollik, S., Long, F., Cheng, P., Wollam, A., Bhonagiri-Palsikar, V., Hallsworth-Pepin, K.,
1221 Clifton, S. W., Weinstock, G. M., & McClelland, M. (2013). Evolutionary Genomics of
1222 Salmonella enterica Subspecies. *MBio*, *4*(2). https://doi.org/10.1128/mBio.00579-12
1223 Diard, M., Bakkeren, E., Cornuault, J. K., Moor, K., Hausmann, A., Sellin, M. E., Loverdo, C., Aertsen,
1224 A., Ackermann, M., De Paepe, M., Slack, E., & Hardt, W. D. (2017). Inflammation boosts
1225 bacteriophage transfer between Salmonella spp. *Science*, *355*(6330), 1211-1215.
1226 https://doi.org/10.1126/science.aaf8451
1227 Diard, M., Sellin, M. E., Dolowschiak, T., Arnoldini, M., Ackermann, M., & Hardt, W. D. (2014).
1228 Antibiotic treatment selects for cooperative virulence of Salmonella typhimurium. *Curr Biol*,
1229 *24*(17), 2000-2005. https://doi.org/10.1016/j.cub.2014.07.028
1230 Endt, K., Maier, L., Kappeli, R., Barthel, M., Misselwitz, B., Kremer, M., & Hardt, W. D. (2012). Peroral
1231 ciprofloxacin therapy impairs the generation of a protective immune response in a mouse
1232 model for Salmonella enterica serovar Typhimurium diarrhea, while parenteral ceftriaxone
1233 therapy does not. *Antimicrob Agents Chemother*, *56*(5), 2295-2304.
1234 https://doi.org/10.1128/AAC.05819-11
1235 Everest, P., Wain, J., Roberts, M., Rook, G., & Dougan, G. (2001). The molecular mechanisms of
1236 severe typhoid fever. *Trends Microbiol*, *9*(7), 316-320. https://doi.org/10.1016/s0966-
1237 842x(01)02067-4
1238 Ghalayini, M., Magnan, M., Dion, S., Zatout, O., Bourguignon, L., Tenaillon, O., & Lescat, M. (2019).
1239 Long-term evolution of the natural isolate of Escherichia coli 536 in the mouse gut colonized
1240 after maternal transmission reveals convergence in the constitutive expression of the lactose
1241 operon. *Mol Ecol*, *28*(19), 4470-4485. https://doi.org/10.1111/mec.15232
1242 Gollan, B., Grabe, G., Michaux, C., & Helaine, S. (2019). Bacterial Persisters and Infection: Past,
1243 Present, and Progressing. *Annu Rev Microbiol*, *73*, 359-385.
1244 https://doi.org/10.1146/annurev-micro-020518-115650
1245 Gonzalez-Escobedo, G., Marshall, J. M., & Gunn, J. S. (2011). Chronic and acute infection of the gall
1246 bladder by Salmonella Typhi: understanding the carrier state. *Nat Rev Microbiol*, *9*(1), 9-14.
1247 https://doi.org/10.1038/nrmicro2490
1248 Grant, A. J., Restif, O., McKinley, T. J., Sheppard, M., Maskell, D. J., & Mastroeni, P. (2008). Modelling
1249 within-host spatiotemporal dynamics of invasive bacterial disease. *PLoS Biol*, *6*(4), e74.
1250 https://doi.org/10.1371/journal.pbio.0060074
1251 Grant, S. S., & Hung, D. T. (2013). Persistent bacterial infections, antibiotic tolerance, and the
1252 oxidative stress response. *Virulence*, *4*(4), 273-283. https://doi.org/10.4161/viru.23987
1253 Habtezion, A., Nguyen, L. P., Hadeiba, H., & Butcher, E. C. (2016). Leukocyte Trafficking to the Small
1254 Intestine and Colon. *Gastroenterology*, *150*(2), 340-354.
1255 https://doi.org/10.1053/j.gastro.2015.10.046
1256 Hapfelmeier, S., Stecher, B., Barthel, M., Kremer, M., Muller, A. J., Heikenwalder, M., Stallmach, T.,
1257 Hensel, M., Pfeffer, K., Akira, S., & Hardt, W. D. (2005). The Salmonella pathogenicity island
1258 (SPI)-2 and SPI-1 type III secretion systems allow Salmonella serovar typhimurium to trigger
1259 colitis via MyD88-dependent and MyD88-independent mechanisms. *J Immunol*, *174*(3), 1675-
1260 1685. http://www.ncbi.nlm.nih.gov/pubmed/15661931

1261 Helaine, S., Cheverton, A. M., Watson, K. G., Faure, L. M., Matthews, S. A., & Holden, D. W. (2014).
1262 Internalization of Salmonella by macrophages induces formation of nonreplicating persisters.
1263 *Science*, *343*(6167), 204-208. https://doi.org/10.1126/science.1244705
1264 Hensel, M., Shea, J. E., Gleeson, C., Jones, M. D., Dalton, E., & Holden, D. W. (1995). Simultaneous
1265 identification of bacterial virulence genes by negative selection. *Science*, *269*(5222), 400-403.
1266 http://www.ncbi.nlm.nih.gov/pubmed/7618105
1267 Hoiseth, S. K., & Stocker, B. A. (1981). Aromatic-dependent *Salmonella* typhimurium are non-virulent
1268 and effective as live vaccines. *Nature*, *291*(5812), 238-239.
1269 http://www.ncbi.nlm.nih.gov/pubmed/7015147
1270 Jarvik, T., Smillie, C., Groisman, E. A., & Ochman, H. (2010). Short-term signatures of evolutionary
1271 change in the Salmonella enterica serovar typhimurium 14028 genome. *J Bacteriol*, *192*(2),
1272 560-567. https://doi.org/10.1128/JB.01233-09
1273 Johnson, P. (2016). *adaptivetau: Tau-Leaping Stochastic Simulation*. R package version 2.2.1.
1274 https://CRAN.R-project.org/package=adaptivetau)
1275 Kaiser, P., Regoes, R. R., Dolowschiak, T., Wotzka, S. Y., Lengefeld, J., Slack, E., Grant, A. J.,
1276 Ackermann, M., & Hardt, W. D. (2014). Cecum lymph node dendritic cells harbor slow-
1277 growing bacteria phenotypically tolerant to antibiotic treatment. *PLoS Biol*, *12*(2), e1001793.
1278 https://doi.org/10.1371/journal.pbio.1001793
1279 Kaiser, P., Slack, E., Grant, A. J., Hardt, W. D., & Regoes, R. R. (2013). Lymph node colonization
1280 dynamics after oral Salmonella Typhimurium infection in mice. *PLoS Pathog*, *9*(9), e1003532.
1281 https://doi.org/10.1371/journal.ppat.1003532
1282 Kreuzer, M., & Hardt, W.-D. (2020). How Food Affects Colonization Resistance Against
1283 Enteropathogenic Bacteria. *Annual Review of Microbiology*, *74*.
1284 Kroger, C., Dillon, S. C., Cameron, A. D., Papenfort, K., Sivasankaran, S. K., Hokamp, K., Chao, Y.,
1285 Sittka, A., Hebrard, M., Handler, K., Colgan, A., Leekitcharoenphon, P., Langridge, G. C.,
1286 Lohan, A. J., Loftus, B., Lucchini, S., Ussery, D. W., Dorman, C. J., Thomson, N. R., Vogel, J., &
1287 Hinton, J. C. (2012). The transcriptional landscape and small RNAs of Salmonella enterica
1288 serovar Typhimurium. *Proc Natl Acad Sci U S A*, *109*(20), E1277-1286.
1289 https://doi.org/10.1073/pnas.1201061109
1290 Lam, L. H., & Monack, D. M. (2014). Intraspecies competition for niches in the distal gut dictate
1291 transmission during persistent Salmonella infection. *PLoS Pathog*, *10*(12), e1004527.
1292 https://doi.org/10.1371/journal.ppat.1004527
1293 Lawley, T. D., Bouley, D. M., Hoy, Y. E., Gerke, C., Relman, D. A., & Monack, D. M. (2008). Host
1294 transmission of Salmonella enterica serovar Typhimurium is controlled by virulence factors
1295 and indigenous intestinal microbiota. *Infect Immun*, *76*(1), 403-416.
1296 https://doi.org/10.1128/IAI.01189-07
1297 Lee, S. M., Donaldson, G. P., Mikulski, Z., Boyajian, S., Ley, K., & Mazmanian, S. K. (2013). Bacterial
1298 colonization factors control specificity and stability of the gut microbiota. *Nature*, *501*(7467),
1299 426-429. https://doi.org/10.1038/nature12447
1300 Leon-Sampedro, R., DelaFuente, J., Diaz-Agero, C., Crellen, T., Musicha, P., Rodriguez-Beltran, J., de la
1301 Vega, C., Hernandez-Garcia, M., Group, R. G. W. S., Lopez-Fresnena, N., Ruiz-Garbajosa, P.,
1302 Canton, R., Cooper, B. S., & San Millan, A. (2021). Pervasive transmission of a carbapenem
1303 resistance plasmid in the gut microbiota of hospitalized patients. *Nat Microbiol*.
1304 https://doi.org/10.1038/s41564-021-00879-y
1305 Levin-Reisman, I., Ronin, I., Gefen, O., Braniss, I., Shoresh, N., & Balaban, N. Q. (2017). Antibiotic
1306 tolerance facilitates the evolution of resistance. *Science*, *355*(6327), 826-830.
1307 https://doi.org/10.1126/science.aaj2191
1308 Liu, J., Gefen, O., Ronin, I., Bar-Meir, M., & Balaban, N. Q. (2020). Effect of tolerance on the evolution
1309 of antibiotic resistance under drug combinations. *Science*, *367*(6474), 200-204.
1310 https://doi.org/10.1126/science.aay3041
1311 Maier, L., Diard, M., Sellin, M. E., Chouffane, E. S., Trautwein-Weidner, K., Periaswamy, B., Slack, E.,
1312 Dolowschiak, T., Stecher, B., Loverdo, C., Regoes, R. R., & Hardt, W. D. (2014). Granulocytes
1313 impose a tight bottleneck upon the gut luminal pathogen population during Salmonella

1314 typhimurium colitis. *PLoS Pathog*, *10*(12), e1004557.
1315 https://doi.org/10.1371/journal.ppat.1004557
1316 Manning, A. J., & Kuehn, M. J. (2011). Contribution of bacterial outer membrane vesicles to innate
1317 bacterial defense. *BMC Microbiol*, *11*, 258. https://doi.org/10.1186/1471-2180-11-258
1318 Marchant, P., Carreno, A., Vivanco, E., Silva, A., Nevermann, J., Otero, C., Araya, E., Gil, F., Calderon, I.
1319 L., & Fuentes, J. A. (2021). "One for All": Functional Transfer of OMV-Mediated Polymyxin B
1320 Resistance From Salmonella enterica sv. Typhi DeltatolR and DeltadegS to Susceptible
1321 Bacteria. *Front Microbiol*, *12*, 672467. https://doi.org/10.3389/fmicb.2021.672467
1322 Marjoram, P., Molitor, J., Plagnol, V., & Tavare, S. (2003). Markov chain Monte Carlo without
1323 likelihoods. *Proc Natl Acad Sci U S A*, *100*(26), 15324-15328.
1324 https://doi.org/10.1073/pnas.0306899100
1325 Martinson, J. N. V., Pinkham, N. V., Peters, G. W., Cho, H., Heng, J., Rauch, M., Broadaway, S. C., &
1326 Walk, S. T. (2019). Rethinking gut microbiome residency and the Enterobacteriaceae in
1327 healthy human adults. *ISME J*, *13*(9), 2306-2318. https://doi.org/10.1038/s41396-019-0435-7
1328 Monack, D. M., Bouley, D. M., & Falkow, S. (2004). Salmonella typhimurium persists within
1329 macrophages in the mesenteric lymph nodes of chronically infected Nramp1+/+ mice and
1330 can be reactivated by IFNgamma neutralization. *J Exp Med*, *199*(2), 231-241.
1331 https://doi.org/10.1084/jem.20031319
1332 Moor, K., Diard, M., Sellin, M. E., Felmy, B., Wotzka, S. Y., Toska, A., Bakkeren, E., Arnoldini, M.,
1333 Bansept, F., Co, A. D., Voller, T., Minola, A., Fernandez-Rodriguez, B., Agatic, G., Barbieri, S.,
1334 Piccoli, L., Casiraghi, C., Corti, D., Lanzavecchia, A., Regoes, R. R., Loverdo, C., Stocker, R.,
1335 Brumley, D. R., Hardt, W. D., & Slack, E. (2017). High-avidity IgA protects the intestine by
1336 enchaining growing bacteria. *Nature*. https://doi.org/10.1038/nature22058
1337 Moor, K., Wotzka, S. Y., Toska, A., Diard, M., Hapfelmeier, S., & Slack, E. (2016). Peracetic Acid
1338 Treatment Generates Potent Inactivated Oral Vaccines from a Broad Range of Culturable
1339 Bacterial Species. *Front Immunol*, *7*, 34. https://doi.org/10.3389/fimmu.2016.00034
1340 Nolivos, S., Cayron, J., Dedieu, A., Page, A., Delolme, F., & Lesterlin, C. (2019). Role of AcrAB-TolC
1341 multidrug efflux pump in drug-resistance acquisition by plasmid transfer. *Science*, *364*(6442),
1342 778-782. https://doi.org/10.1126/science.aav6390
1343 Onwuezobe, I. A., Oshun, P. O., & Odigwe, C. C. (2012). Antimicrobials for treating symptomatic non-
1344 typhoidal Salmonella infection. *Cochrane Database Syst Rev*, *11*, CD001167.
1345 https://doi.org/10.1002/14651858.CD001167.pub2
1346 Perlin, M. H., Clark, D. R., McKenzie, C., Patel, H., Jackson, N., Kormanik, C., Powell, C., Bajorek, A.,
1347 Myers, D. A., Dugatkin, L. A., & Atlas, R. M. (2009). Protection of Salmonella by ampicillin-
1348 resistant Escherichia coli in the presence of otherwise lethal drug concentrations. *Proc Biol*
1349 *Sci*, *276*(1674), 3759-3768. https://doi.org/10.1098/rspb.2009.0997
1350 Pham, T. H. M., Brewer, S. M., Thurston, T., Massis, L. M., Honeycutt, J., Lugo, K., Jacobson, A. R.,
1351 Vilches-Moure, J. G., Hamblin, M., Helaine, S., & Monack, D. M. (2020). Salmonella-Driven
1352 Polarization of Granuloma Macrophages Antagonizes TNF-Mediated Pathogen Restriction
1353 during Persistent Infection. *Cell Host Microbe*, *27*(1), 54-67 e55.
1354 https://doi.org/10.1016/j.chom.2019.11.011
1355 Rosenberg, G., Yehezkel, D., Hoffman, D., Mattioli, C. C., Fremder, M., Ben-Arosh, H., Vainman, L.,
1356 Nissani, N., Hen-Avivi, S., Brenner, S., Itkin, M., Malitsky, S., Ohana, E., Ben-Moshe, N. B., &
1357 Avraham, R. (2021). Host succinate is an activation signal for Salmonella virulence during
1358 intracellular infection. *Science*, *371*(6527), 400-405. https://doi.org/10.1126/science.aba8026
1359 San Roman, B., Garrido, V., Sanchez, S., Martinez-Ballesteros, I., Garaizar, J., Mainar-Jaime, R. C.,
1360 Migura-Garcia, L., & Grillo, M. J. (2018). Relationship between Salmonella infection, shedding
1361 and serology in fattening pigs in low-moderate prevalence areas. *Zoonoses Public Health*,
1362 *65*(5), 481-489. https://doi.org/10.1111/zph.12453
1363 Stapels, D. A. C., Hill, P. W. S., Westermann, A. J., Fisher, R. A., Thurston, T. L., Saliba, A. E.,
1364 Blommestein, I., Vogel, J., & Helaine, S. (2018). Salmonella persisters undermine host
1365 immune defenses during antibiotic treatment. *Science*, *362*(6419), 1156-1160.
1366 https://doi.org/10.1126/science.aat7148

1367 Stecher, B., Chaffron, S., Kappeli, R., Hapfelmeier, S., Freedrich, S., Weber, T. C., Kirundi, J., Suar, M.,
1368 McCoy, K. D., von Mering, C., Macpherson, A. J., & Hardt, W. D. (2010). Like will to like:
1369 abundances of closely related species can predict susceptibility to intestinal colonization by
1370 pathogenic and commensal bacteria. *PLoS Pathog*, *6*(1), e1000711.
1371 https://doi.org/10.1371/journal.ppat.1000711
1372 Stecher, B., Denzler, R., Maier, L., Bernet, F., Sanders, M. J., Pickard, D. J., Barthel, M., Westendorf, A.
1373 M., Krogfelt, K. A., Walker, A. W., Ackermann, M., Dobrindt, U., Thomson, N. R., & Hardt, W.
1374 D. (2012). Gut inflammation can boost horizontal gene transfer between pathogenic and
1375 commensal Enterobacteriaceae. *Proc Natl Acad Sci U S A*, *109*(4), 1269-1274.
1376 https://doi.org/10.1073/pnas.1113246109
1377 Stecher, B., & Hardt, W. D. (2011). Mechanisms controlling pathogen colonization of the gut. *Curr*
1378 *Opin Microbiol*, *14*(1), 82-91. https://doi.org/10.1016/j.mib.2010.10.003
1379 Stecher, B., Paesold, G., Barthel, M., Kremer, M., Jantsch, J., Stallmach, T., Heikenwalder, M., &
1380 Hardt, W. D. (2006). Chronic Salmonella enterica serovar Typhimurium-induced colitis and
1381 cholangitis in streptomycin-pretreated Nramp1+/+ mice. *Infect Immun*, *74*(9), 5047-5057.
1382 https://doi.org/10.1128/IAI.00072-06
1383 Stecher, B., Robbiani, R., Walker, A. W., Westendorf, A. M., Barthel, M., Kremer, M., Chaffron, S.,
1384 Macpherson, A. J., Buer, J., Parkhill, J., Dougan, G., von Mering, C., & Hardt, W. D. (2007).
1385 Salmonella enterica serovar typhimurium exploits inflammation to compete with the
1386 intestinal microbiota. *PLoS Biol*, *5*(10), 2177-2189.
1387 https://doi.org/10.1371/journal.pbio.0050244
1388 Sternberg, N. L., & Maurer, R. (1991). Bacteriophage-mediated generalized transduction in
1389 Escherichia coli and Salmonella typhimurium. *Methods Enzymol*, *204*, 18-43.
1390 http://www.ncbi.nlm.nih.gov/pubmed/1943777
1391 Temkin, E., Adler, A., Lerner, A., & Carmeli, Y. (2014). Carbapenem-resistant Enterobacteriaceae:
1392 biology, epidemiology, and management. *Ann N Y Acad Sci*, *1323*, 22-42.
1393 https://doi.org/10.1111/nyas.12537
1394 Tenaillon, O., Skurnik, D., Picard, B., & Denamur, E. (2010). The population genetics of commensal
1395 Escherichia coli. *Nat Rev Microbiol*, *8*(3), 207-217. https://doi.org/10.1038/nrmicro2298
1396 Tschudin-Sutter, S., Frei, R., Schwahn, F., Tomic, M., Conzelmann, M., Stranden, A., & Widmer, A. F.
1397 (2016). Prospective Validation of Cessation of Contact Precautions for Extended-Spectrum
1398 beta-Lactamase-Producing Escherichia coli(1). *Emerg Infect Dis*, *22*(6), 1094-1097.
1399 https://doi.org/10.3201/eid2206.150554
1400 Van Boeckel, T. P., Pires, J., Silvester, R., Zhao, C., Song, J., Criscuolo, N. G., Gilbert, M., Bonhoeffer, S.,
1401 & Laxminarayan, R. (2019). Global trends in antimicrobial resistance in animals in low- and
1402 middle-income countries. *Science*, *365*(6459). https://doi.org/10.1126/science.aaw1944
1403 WHO. (2014). *Antimicrobial resistance: global report on surveillance*. World Health Organization
1404 (WHO).
1405 WHO. (2017). *Global priority list of antibiotic-resistant bacteria to guide research, discovery, and*
1406 *development of new antibiotics*. WHO (World Health Organization).
1407 Windels, E. M., Michiels, J. E., Fauvart, M., Wenseleers, T., Van den Bergh, B., & Michiels, J. (2019).
1408 Bacterial persistence promotes the evolution of antibiotic resistance by increasing survival
1409 and mutation rates. *ISME J*, *13*(5), 1239-1251. https://doi.org/10.1038/s41396-019-0344-9
1410 Wirfs, M. J. (2019). *The APRN and PA's Complete Guide to Prescribing Drug Therapy 2020*. Springer
1411 Publishing Company.
1412 Wotzka, S. Y., Kreuzer, M., Maier, L., Arnoldini, M., Nguyen, B. D., Brachmann, A. O., Berthold, D. L.,
1413 Zund, M., Hausmann, A., Bakkeren, E., Hoces, D., Gul, E., Beutler, M., Dolowschiak, T.,
1414 Zimmermann, M., Fuhrer, T., Moor, K., Sauer, U., Typas, A., Piel, J., Diard, M., Macpherson, A.
1415 J., Stecher, B., Sunagawa, S., Slack, E., & Hardt, W. D. (2019). Escherichia coli limits
1416 Salmonella Typhimurium infections after diet shifts and fat-mediated microbiota
1417 perturbation in mice. *Nat Microbiol*. https://doi.org/10.1038/s41564-019-0568-5
1418 Wright, G. D. (2007). The antibiotic resistome: the nexus of chemical and genetic diversity. *Nat Rev*
1419 *Microbiol*, *5*(3), 175-186. https://doi.org/10.1038/nrmicro1614

1420 Yang, D., Guo, Y., & Zhang, Z. (2009). Combined porin loss and extended spectrum beta-lactamase
1421 production is associated with an increasing imipenem minimal inhibitory concentration in
1422 clinical Klebsiella pneumoniae strains. *Curr Microbiol*, *58*(4), 366-370.
1423 https://doi.org/10.1007/s00284-009-9364-4

1424

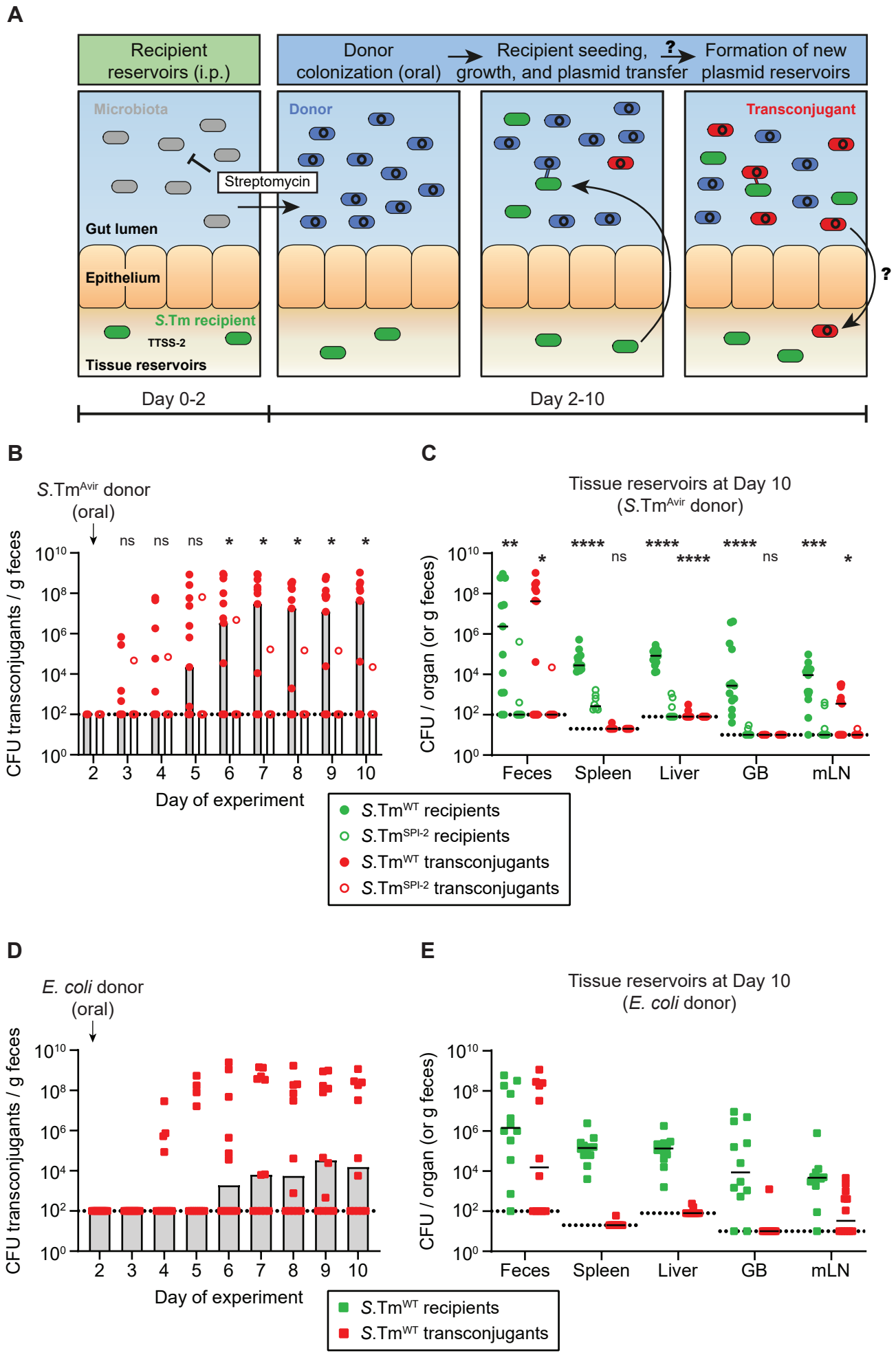

Bakkeren et al. Figure 1

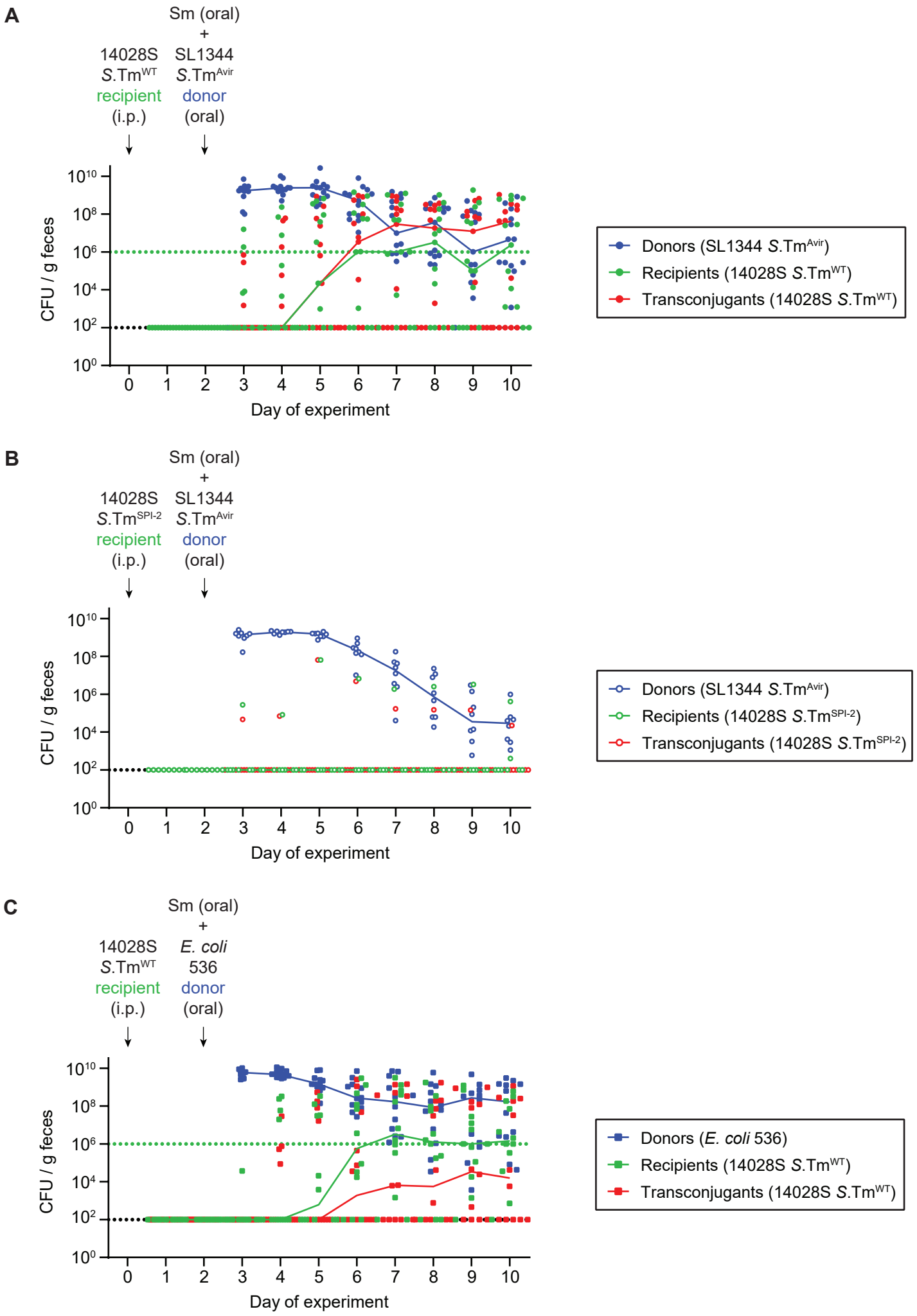

Bakkeren et al. Figure 1-figure supplement 1

14028S (recipient) chromosome-specific PCR

(221bp expected size)

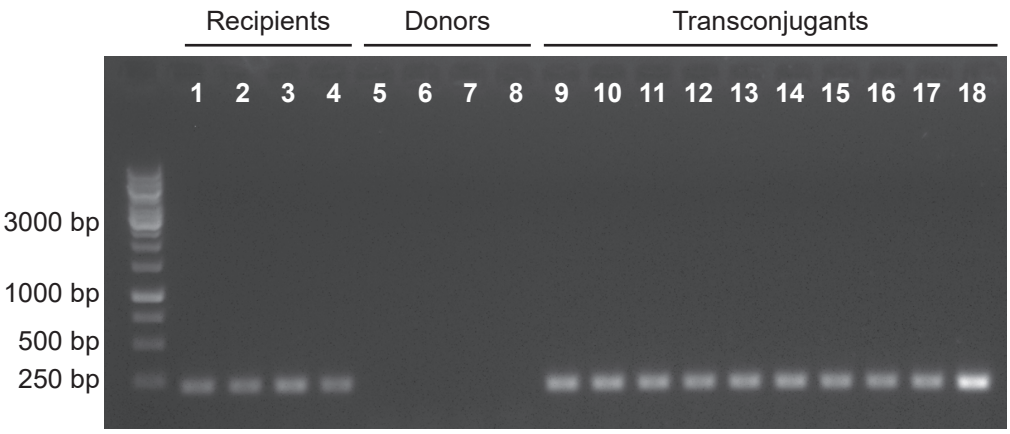

P2^{cat}-specific PCR

(535bp expected size)

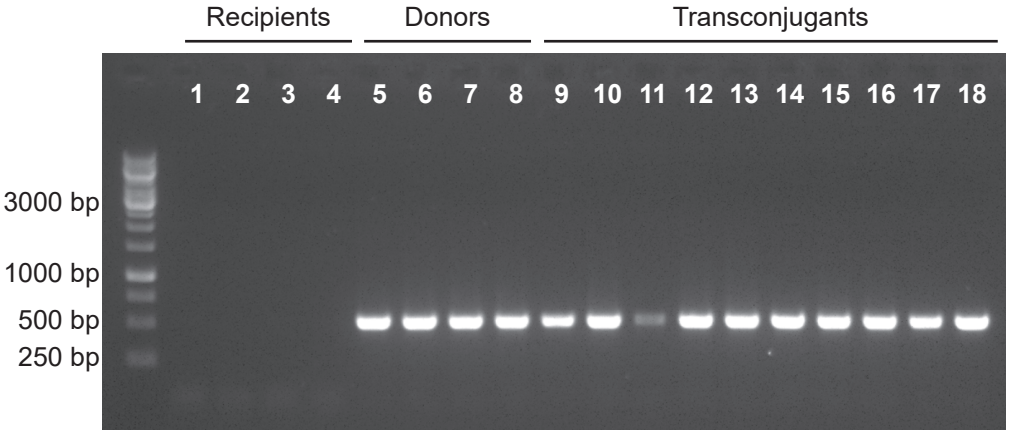

Lane #	Mouse #	Site of isolation	Day of isolation	Resist-ance
1	1	mLN	10	Kan
2	2	mLN	10	Kan
3	1	Feces	10	Kan
4	2	Feces	10	Kan
5	7	mLN	10	Cm
6	8	mLN	10	Cm
7	7	Feces	10	Cm
8	8	Feces	10	Cm
9	6	mLN	10	Kan+Cm
10	6	mLN	10	Kan+Cm
11	6	mLN	10	Kan+Cm
12	6	mLN	10	Kan+Cm
13	6	mLN	10	Kan+Cm
14	6	Feces	10	Kan+Cm
15	6	Feces	10	Kan+Cm
16	6	Feces	10	Kan+Cm
17	6	Feces	10	Kan+Cm
18	6	Feces	10	Kan+Cm

Bakkeren et al. Figure 1-figure supplement 2

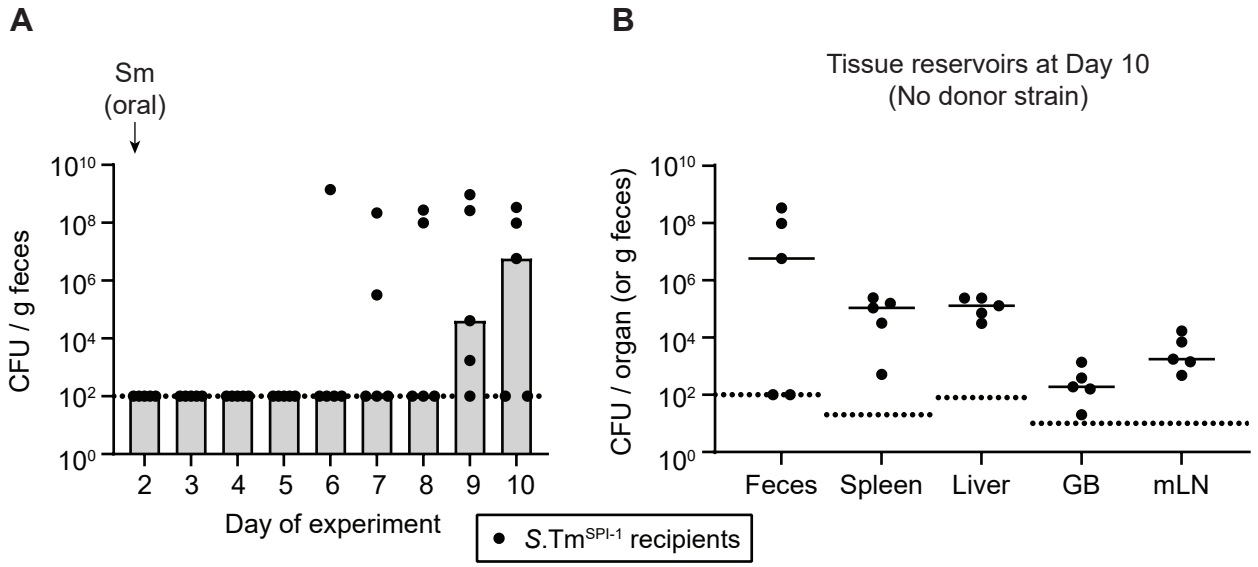

Bakkeren et al. Figure 1-figure supplement 3

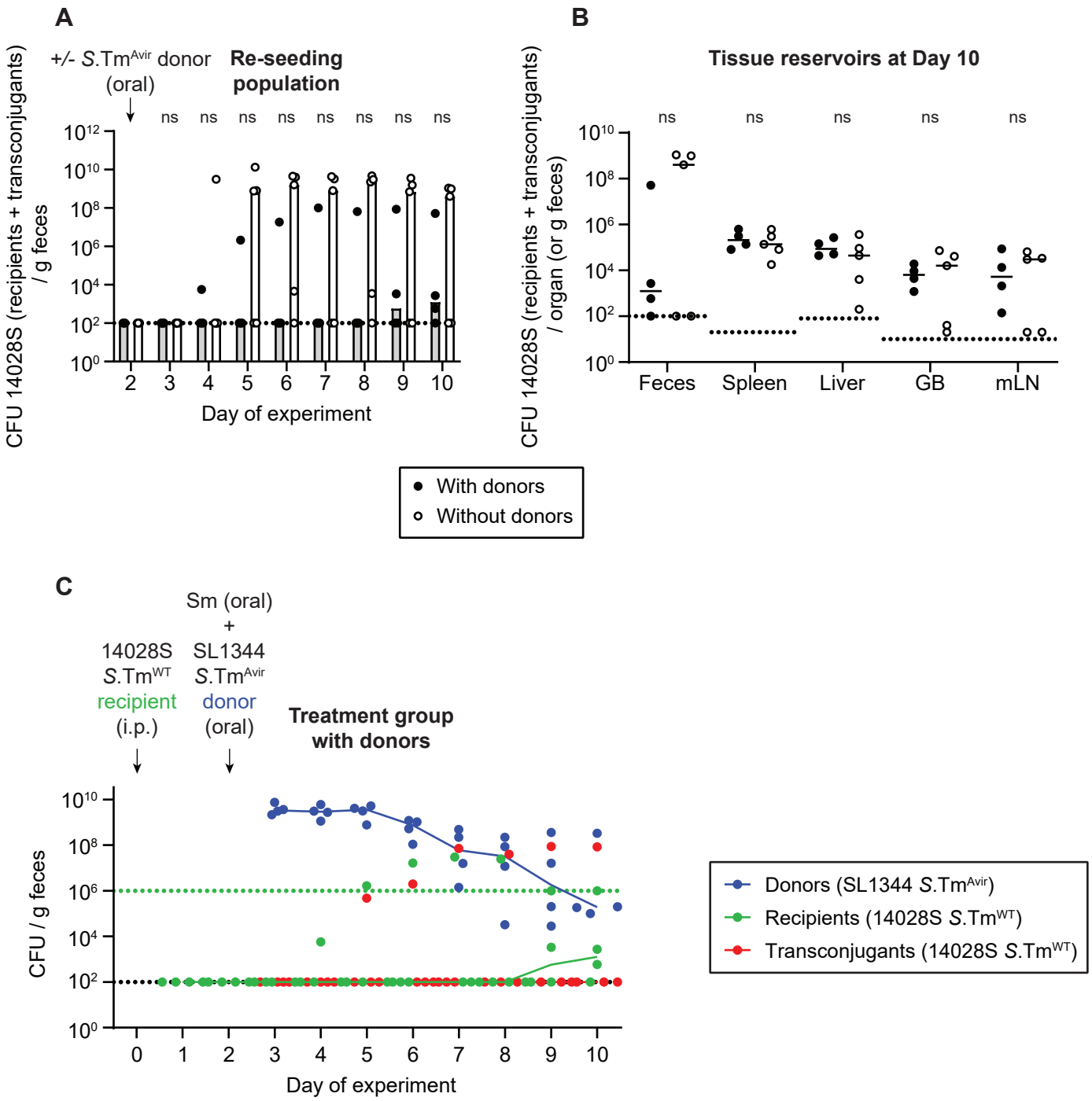

Bakkeren et al. Figure 1-figure supplement 4

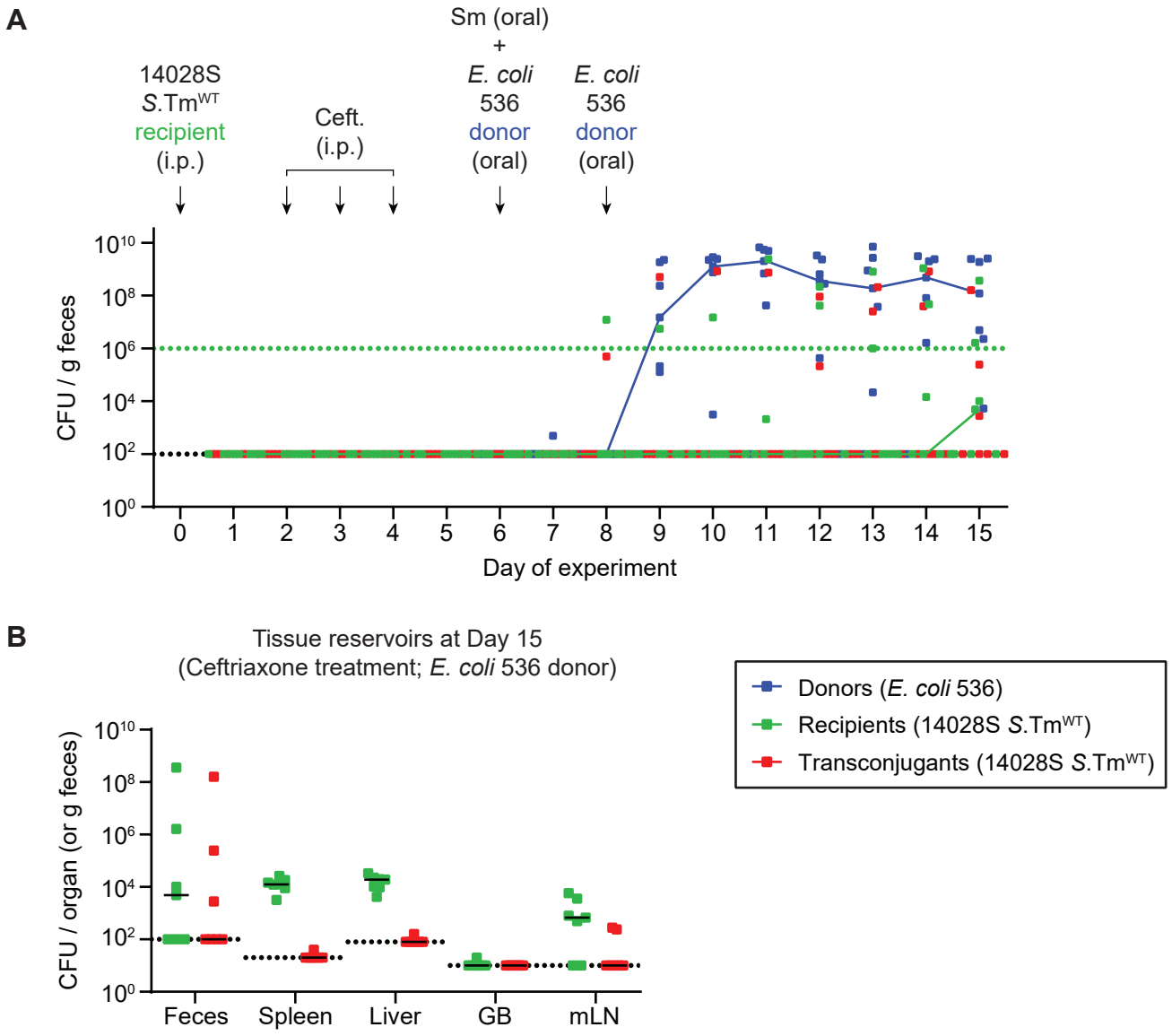

Bakkeren et al. Figure 1-figure supplement 5

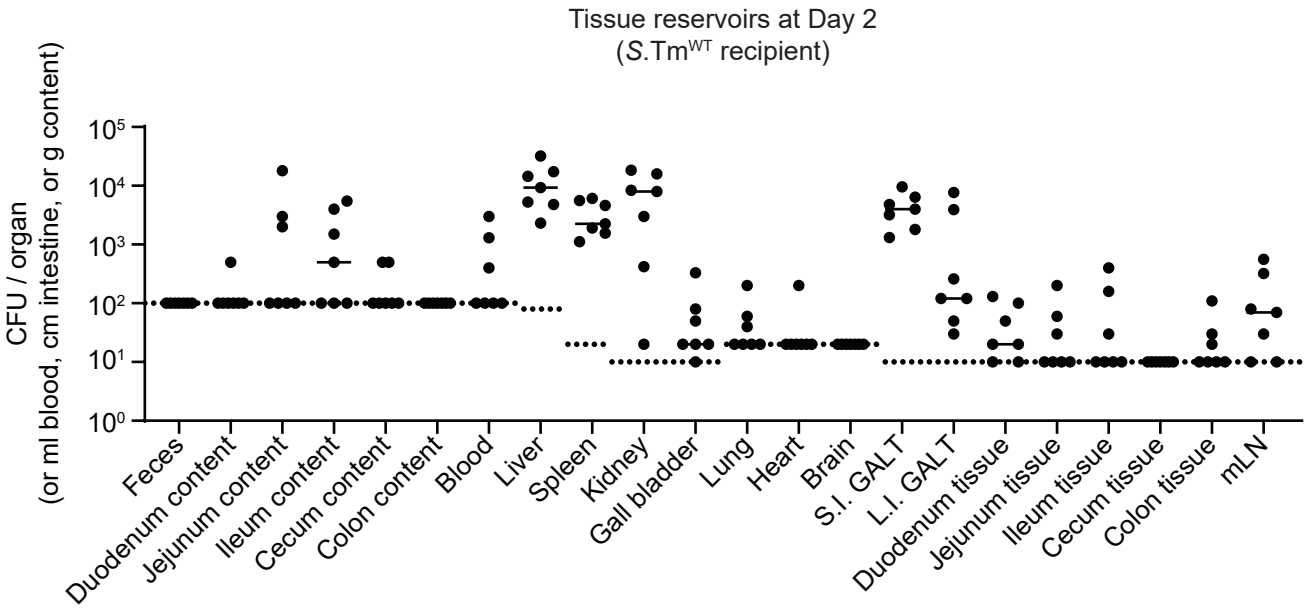

Bakkeren et al. Figure 1-figure supplement 6

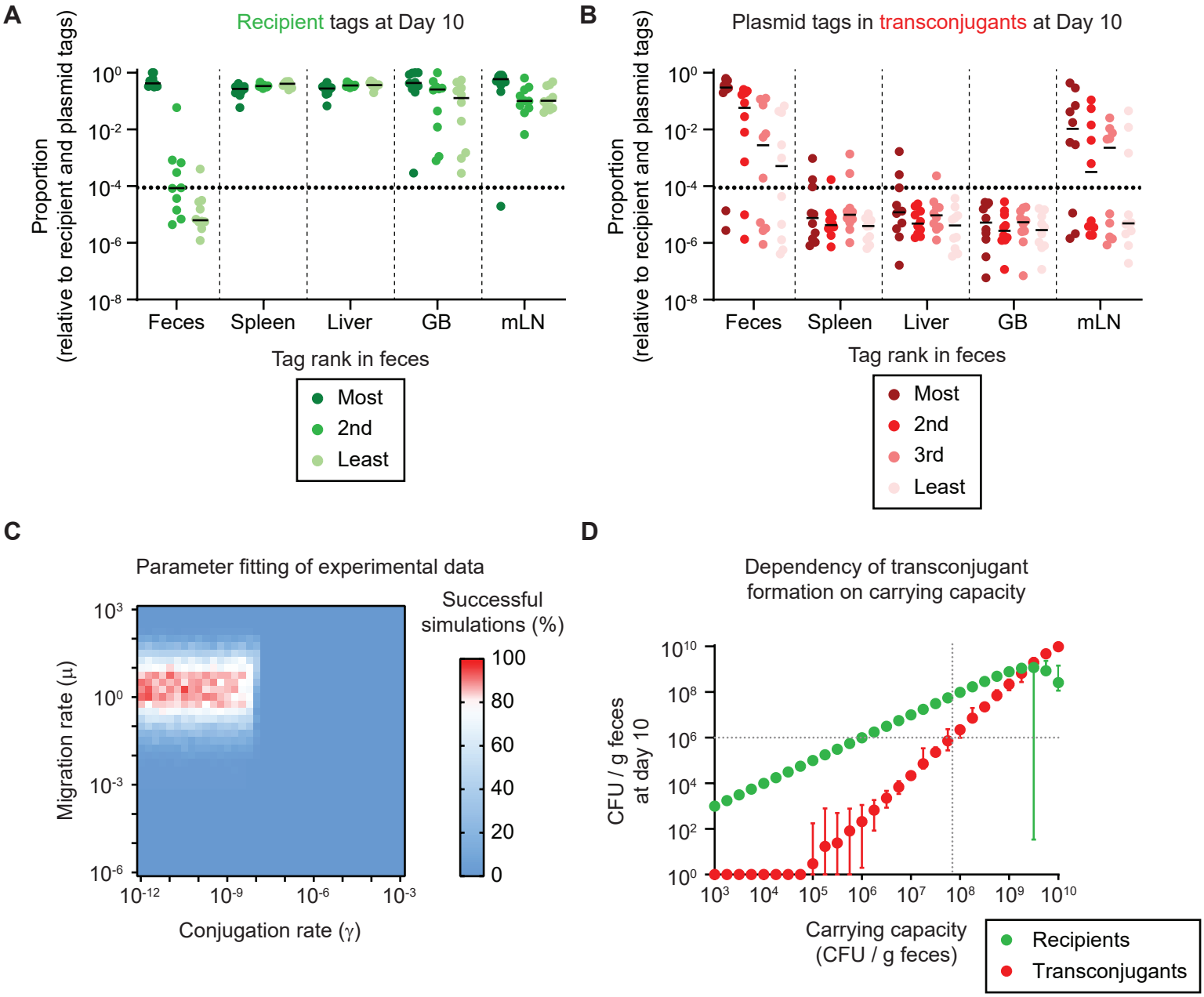

Bakkeren et al. Figure 2

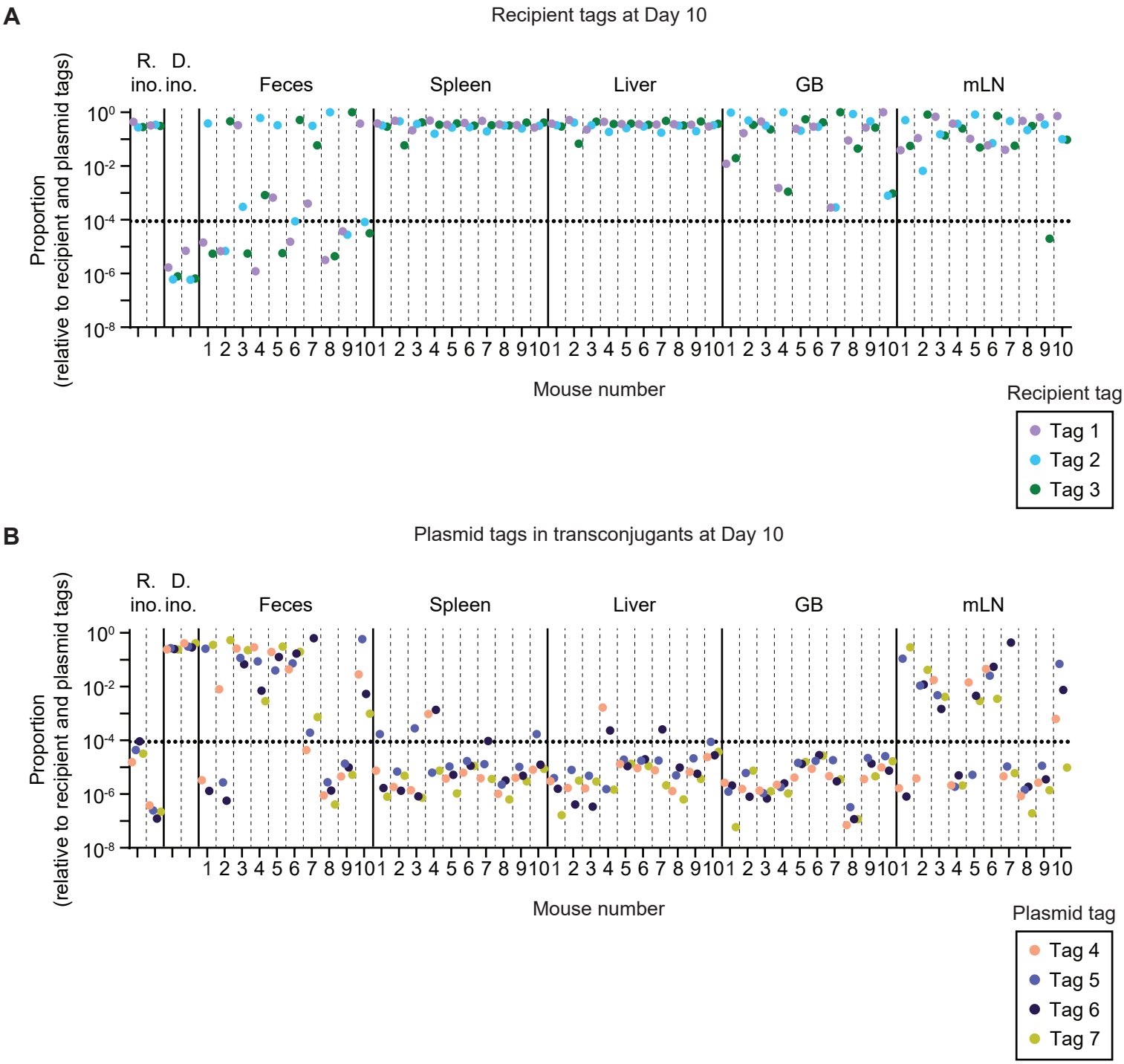

Bakkeren et al. Figure 2-figure supplement 1

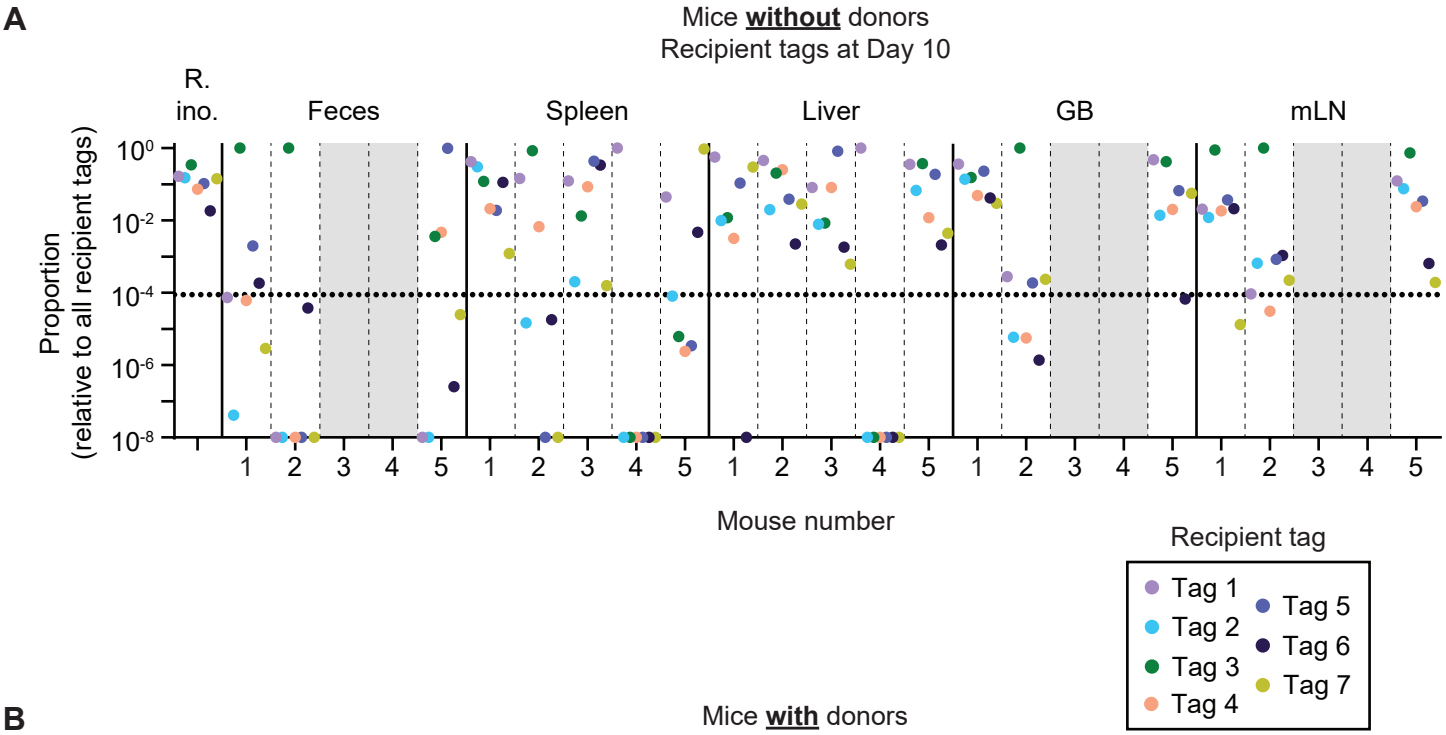

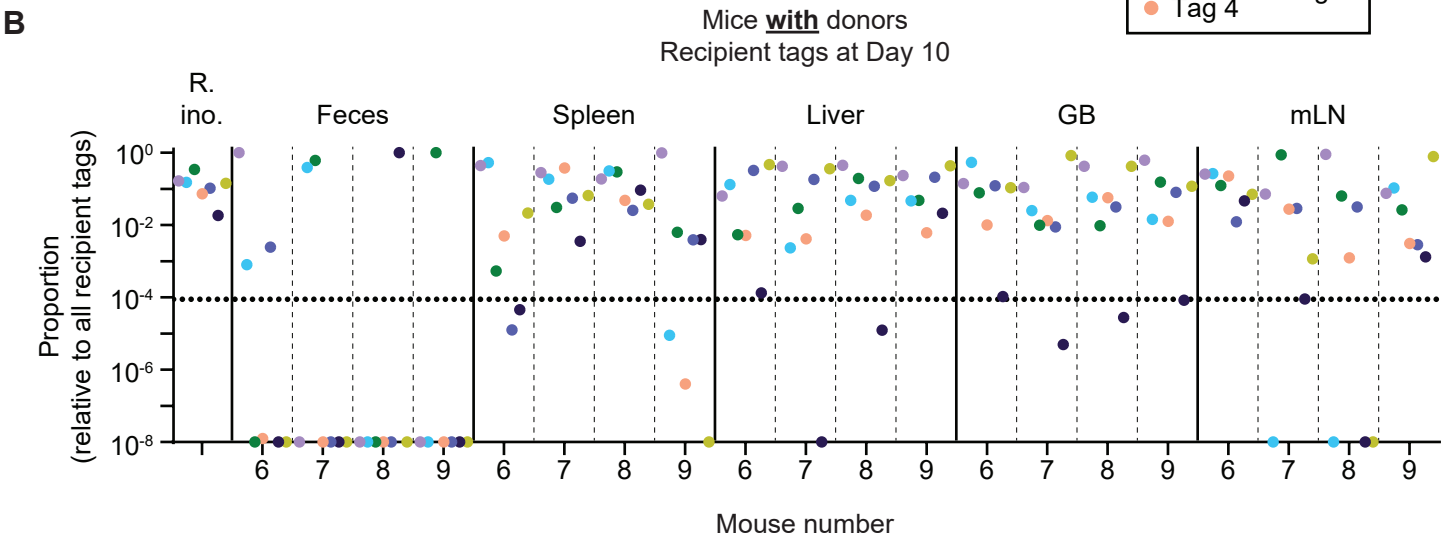

Bakkeren et al. Figure 2-figure supplement 2

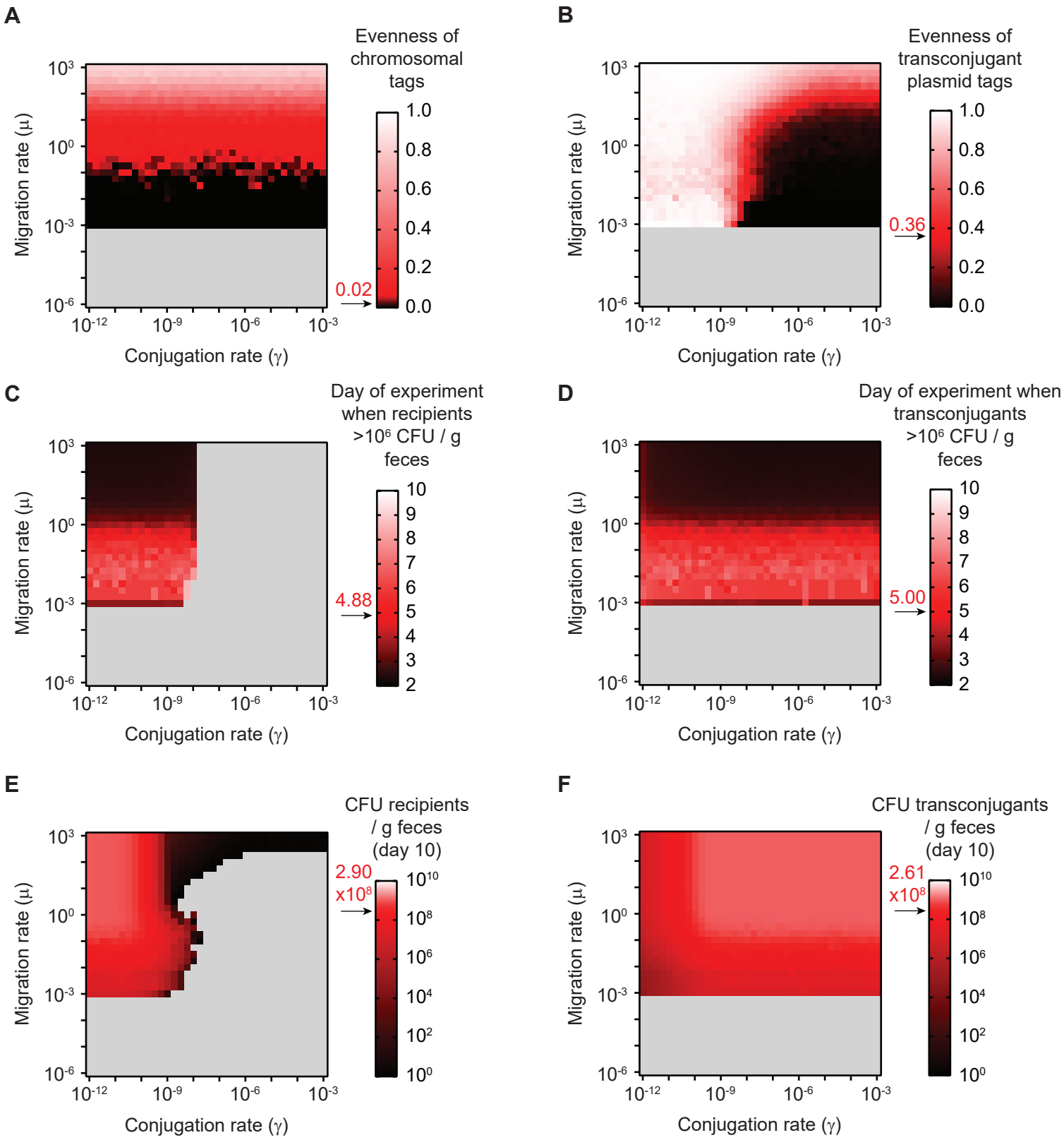

Bakkeren et al. Figure 2-figure supplement 3

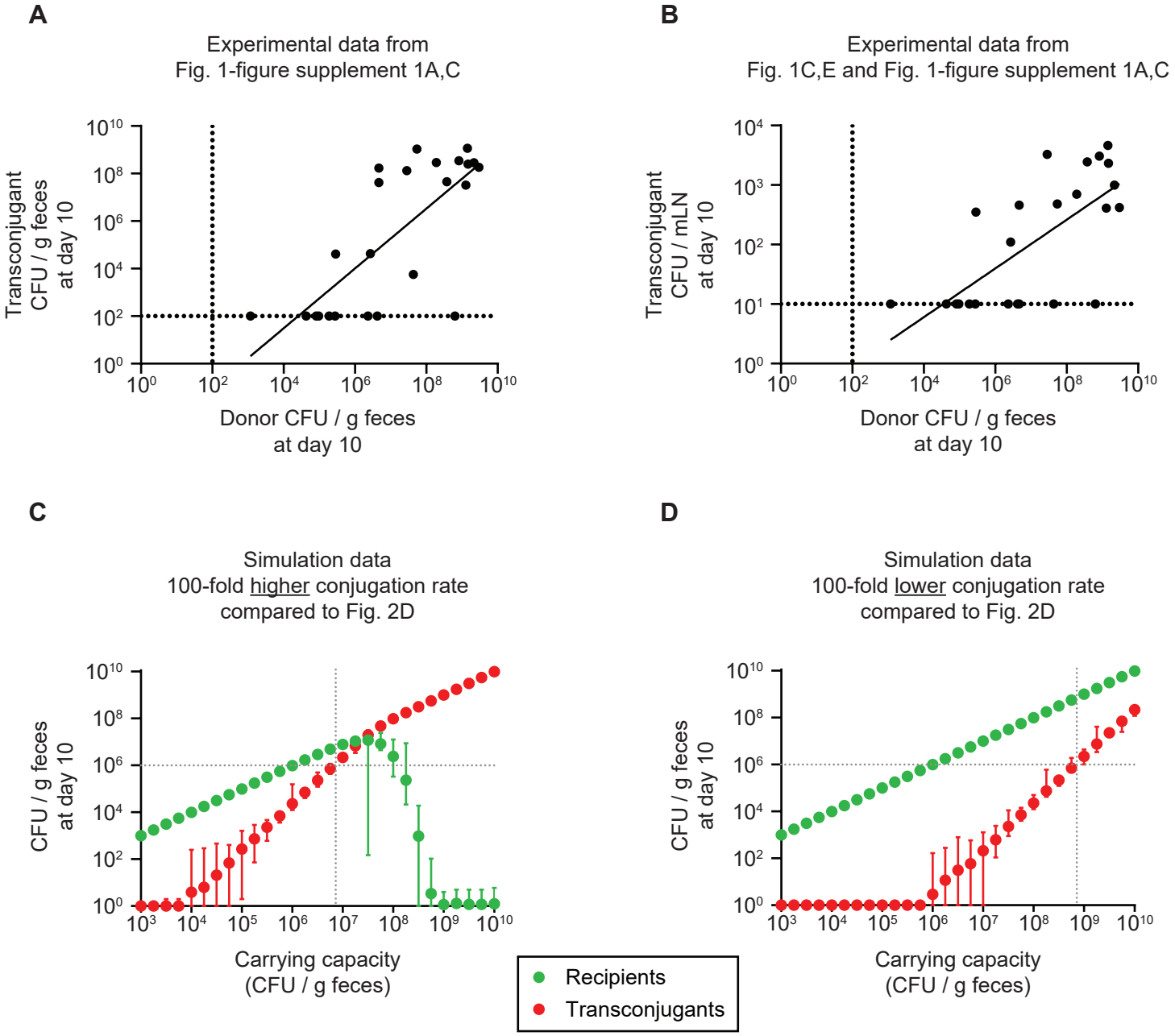

Bakkeren et al. Figure 2-figure supplement 4

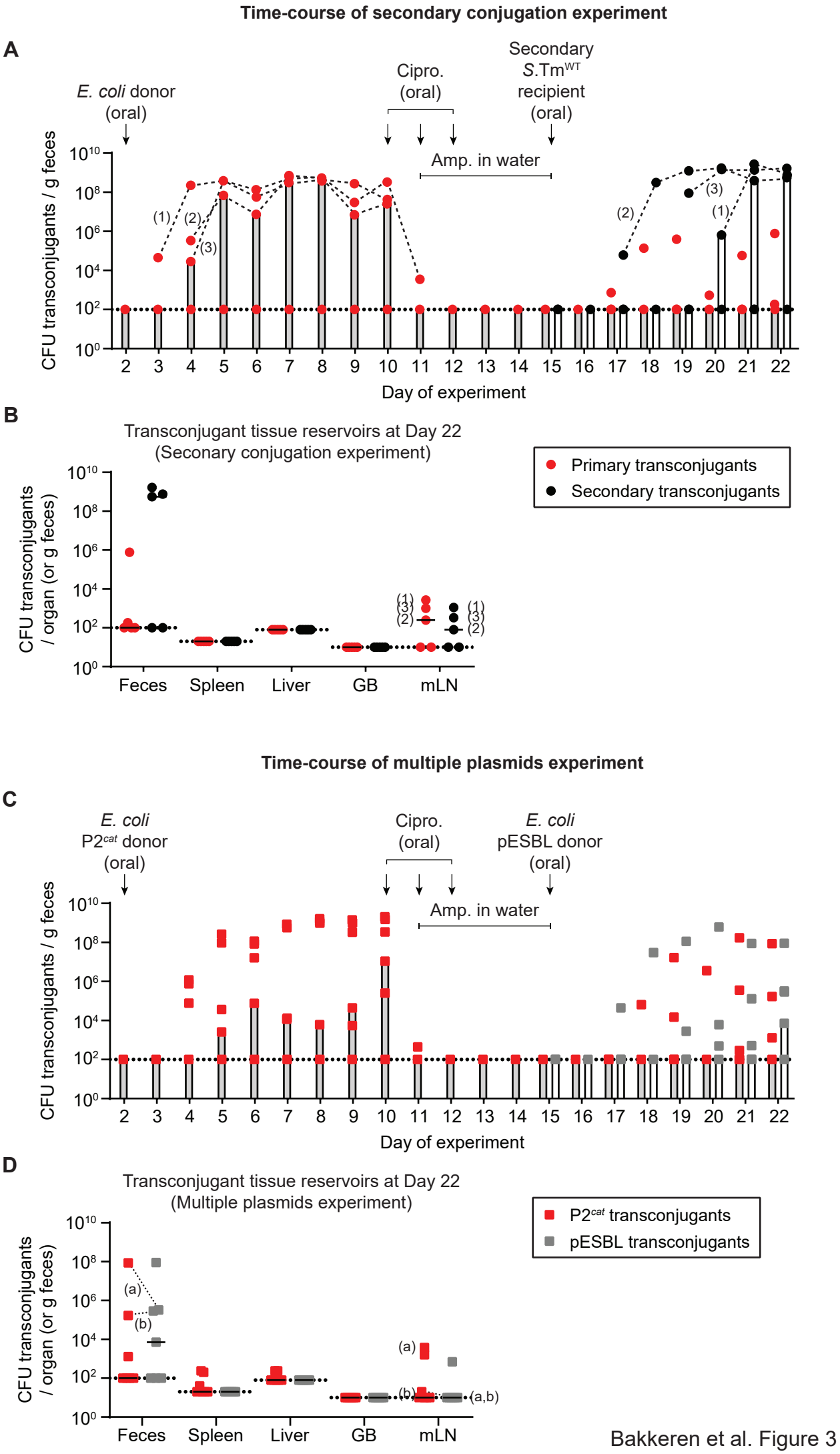

Bakkeren et al. Figure 3

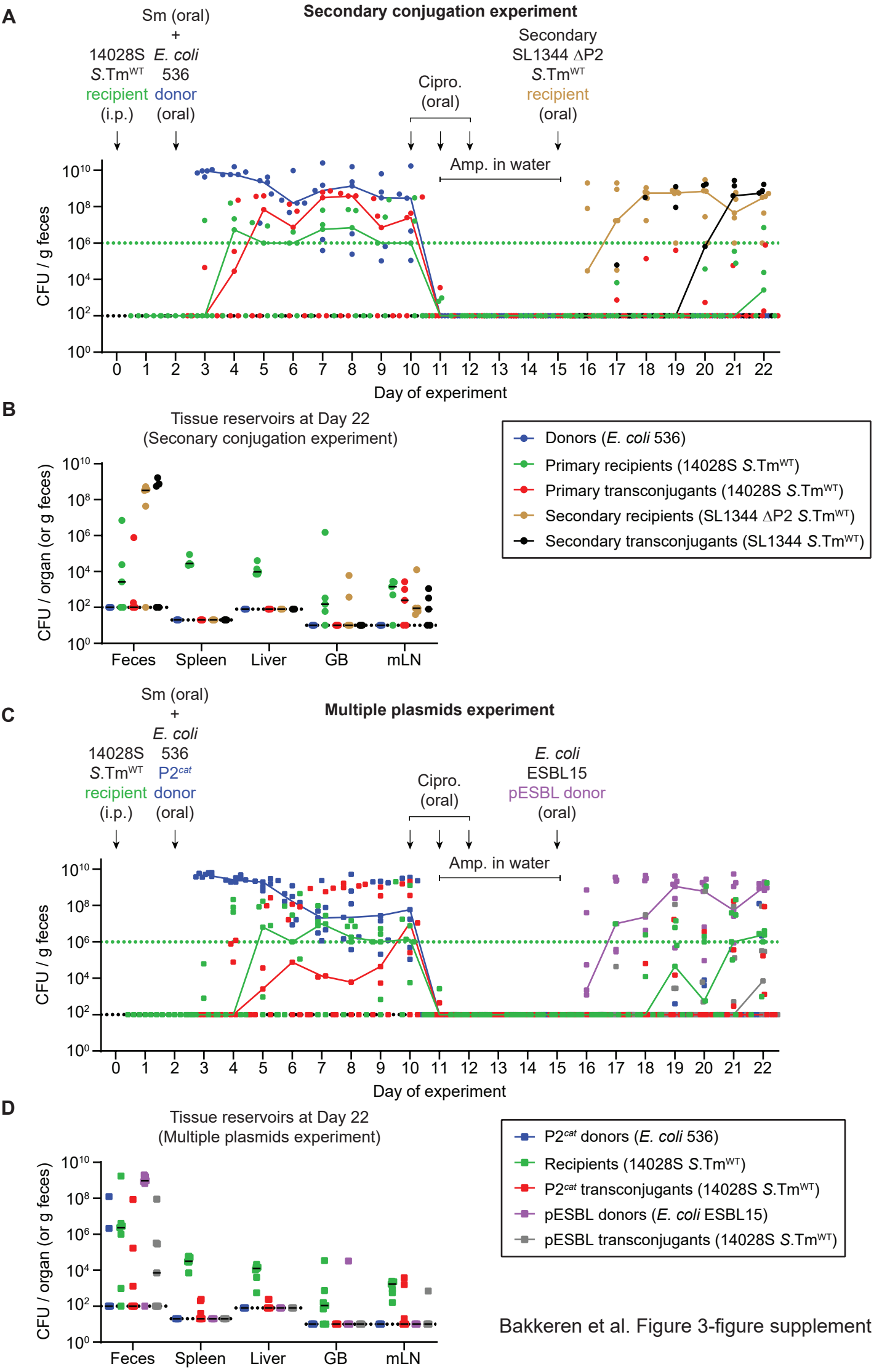

Bakkeren et al. Figure 3-figure supplement 1

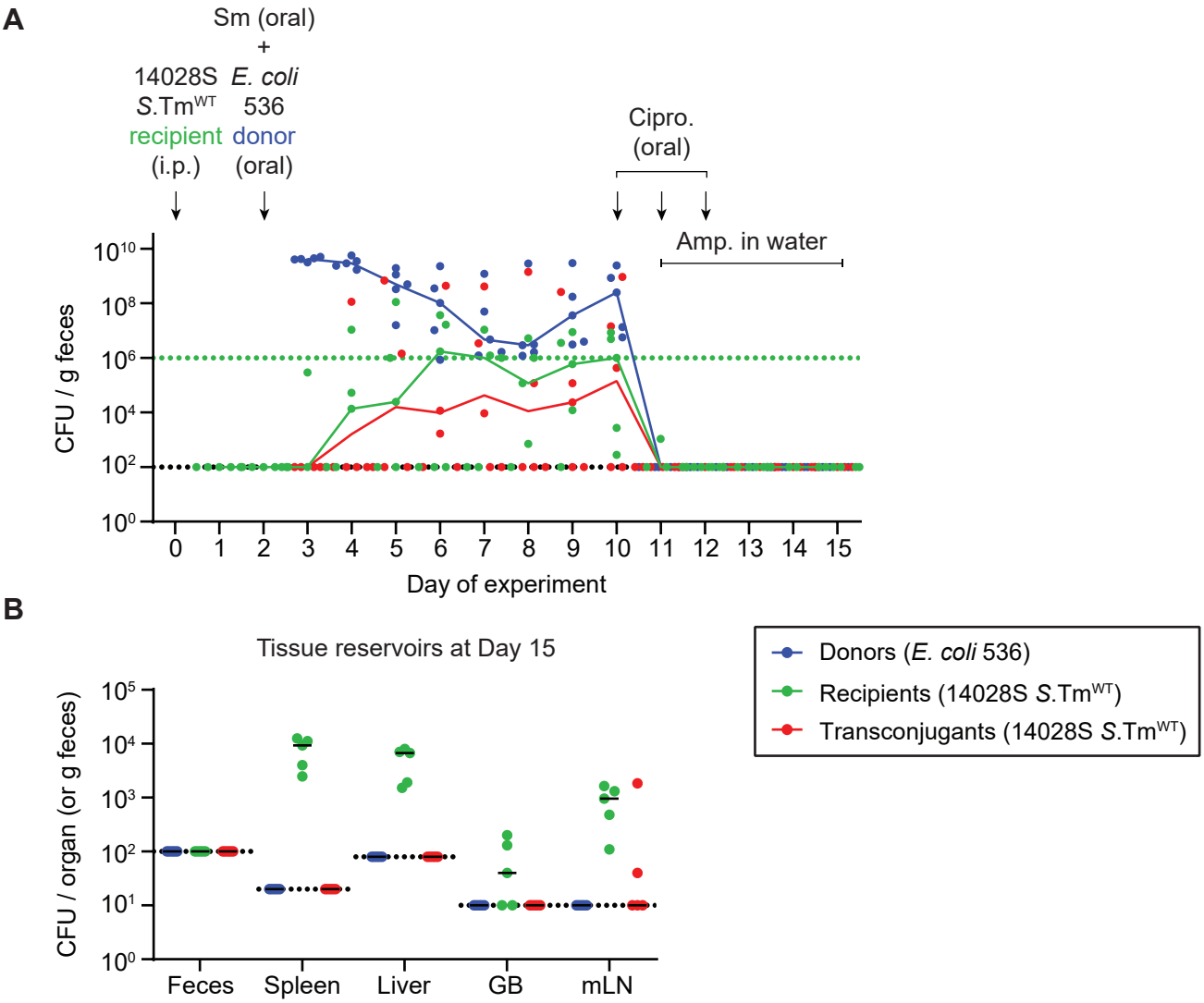

Bakkeren et al. Figure 3-figure supplement 2

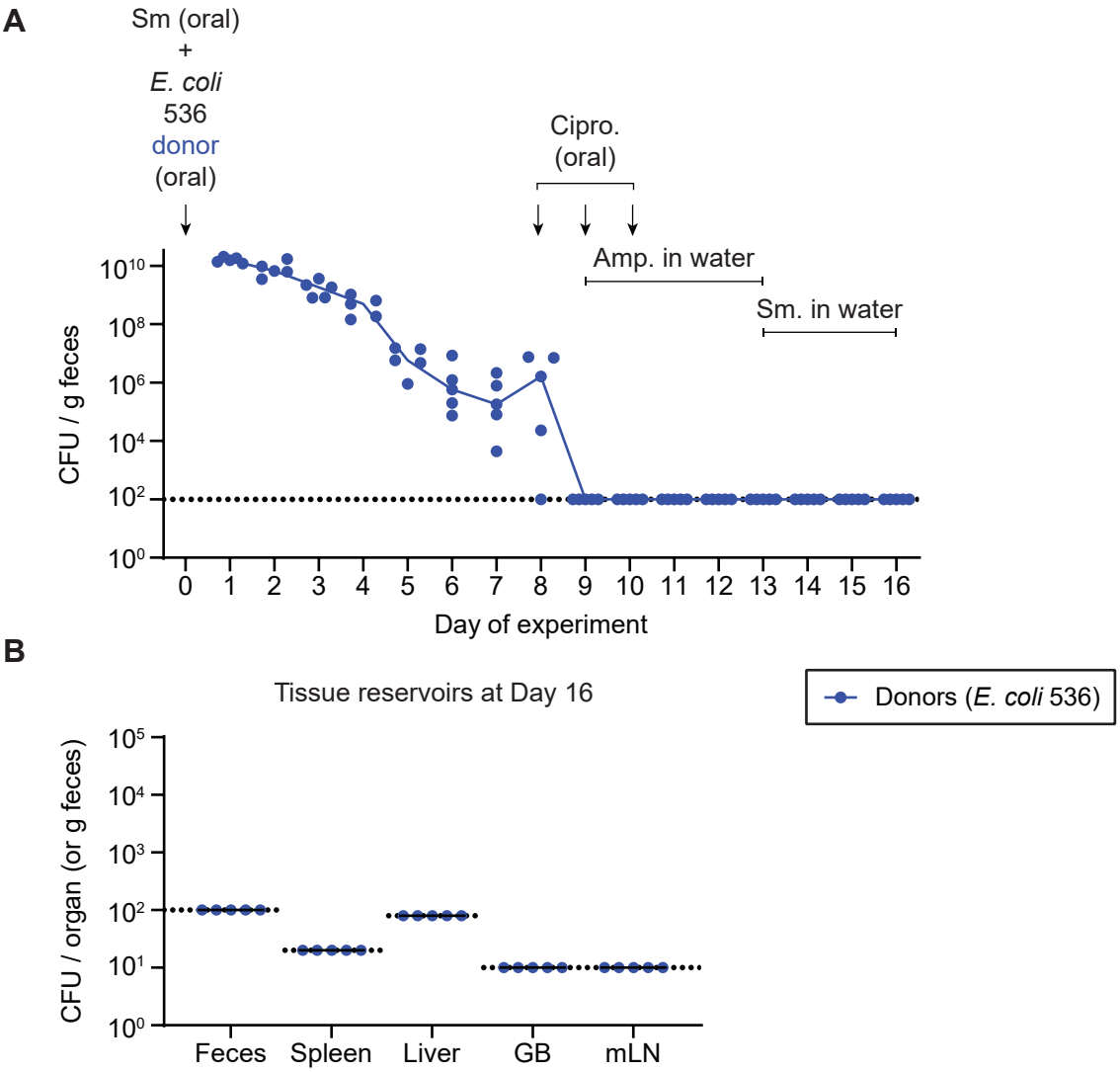

Bakkeren et al. Figure 3-figure supplement 3

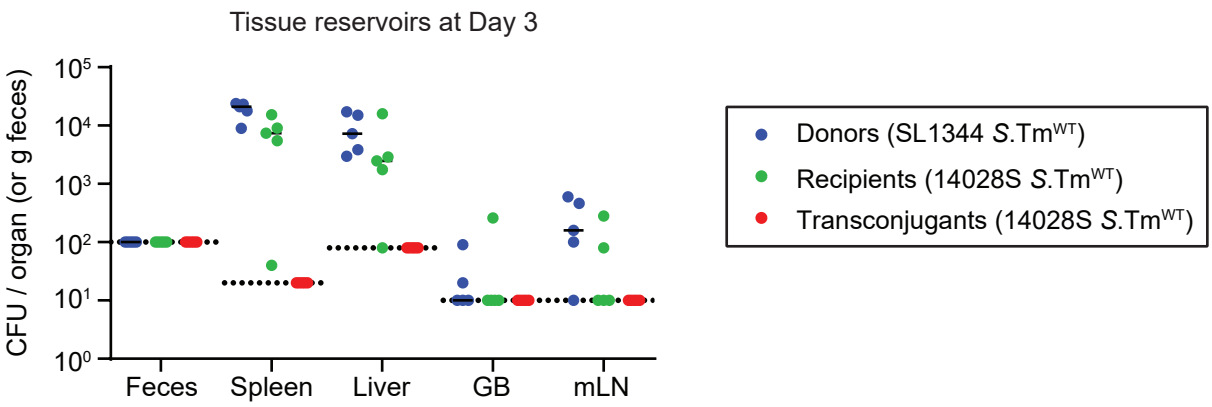

Bakkeren et al. Figure 3-figure supplement 4

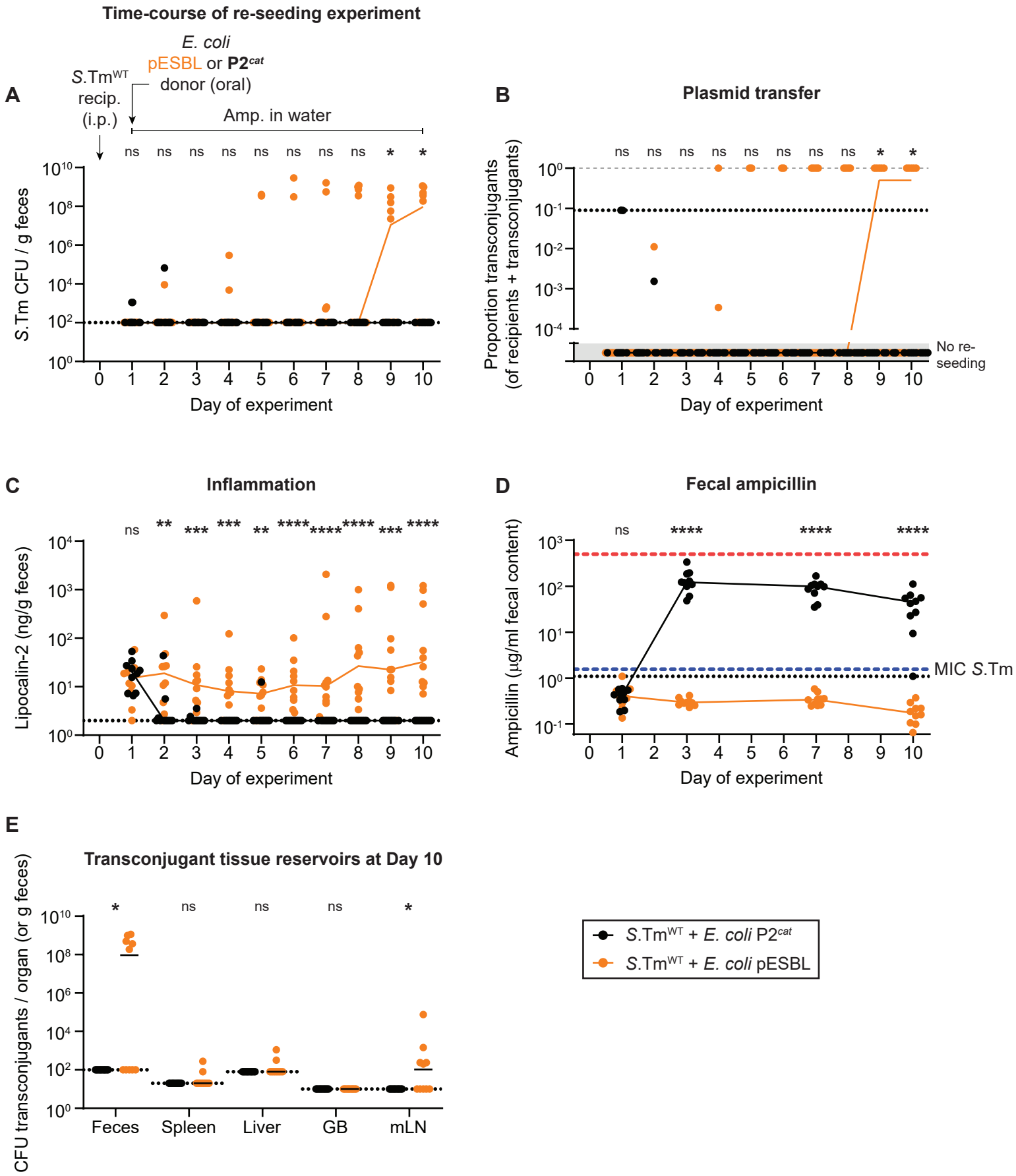

Bakkeren et al. Figure 4

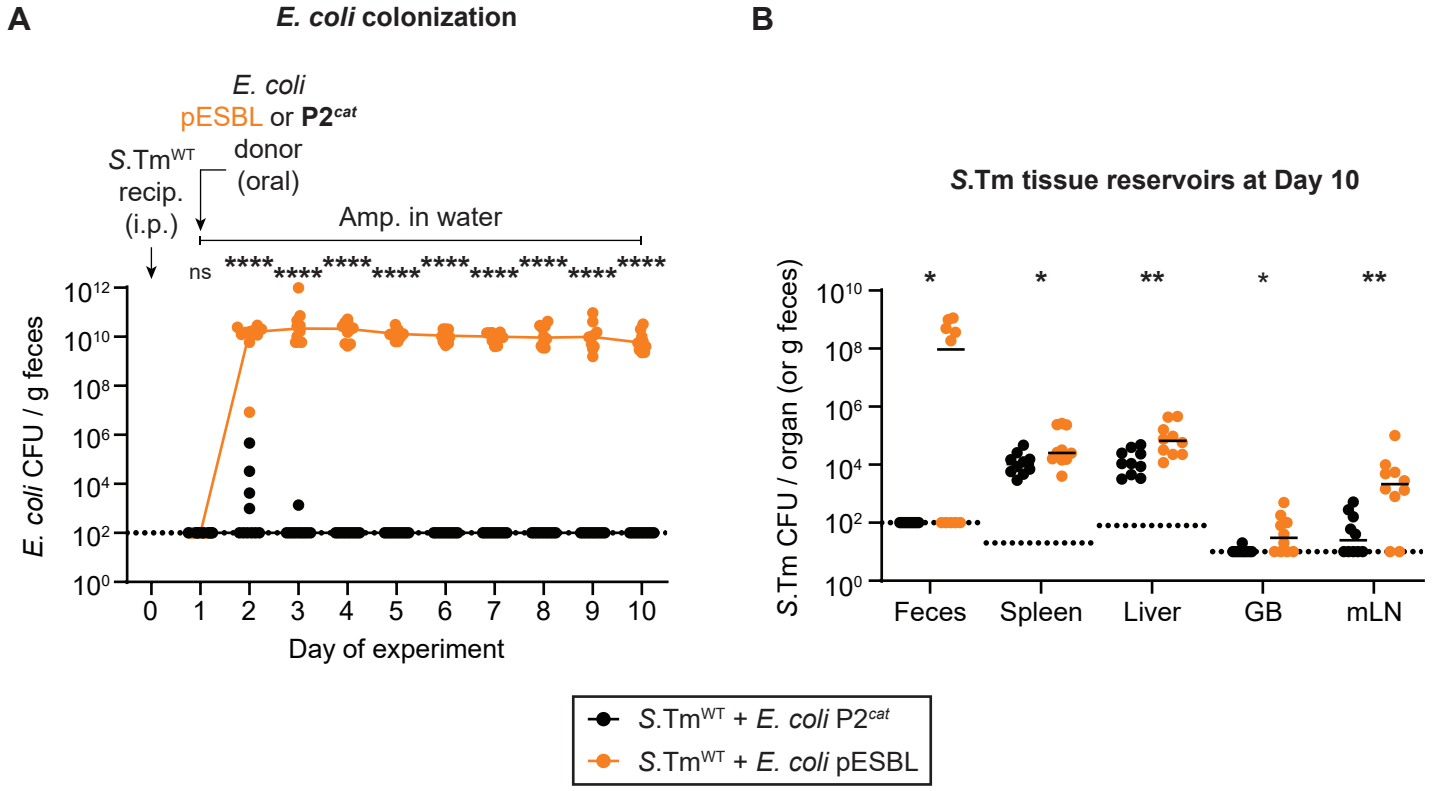

Bakkeren et al. Figure 4-figure supplement 1

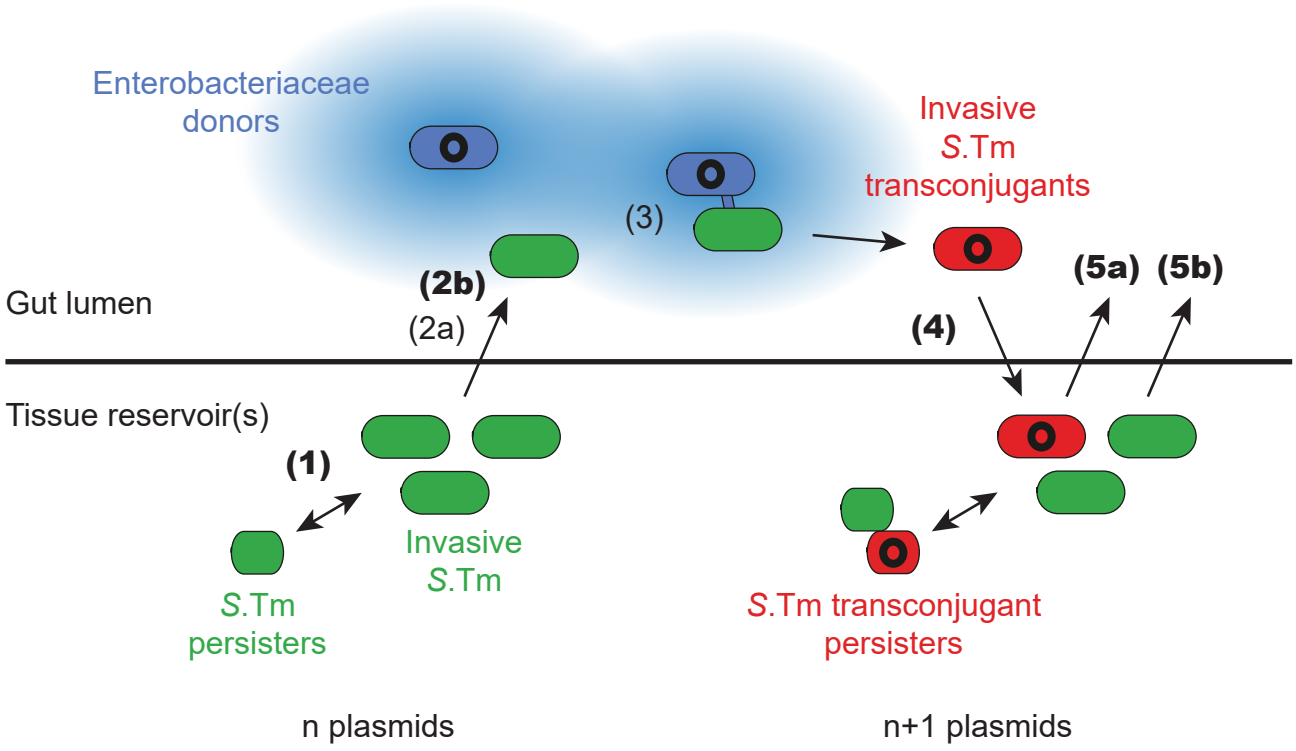

Bakkeren et al. Figure 5